

1 **MAML1-induced HPV E6 oncoprotein stability is required for cellular proliferation and**  
2 **migration of cervical tumor-derived cells**

3

4 Josipa Skelin<sup>1\*</sup>, Anamaria Đukić<sup>1\*</sup>, Vedrana Filić<sup>2</sup>, Martin Hufbauer<sup>3</sup>, Baki Akgül<sup>3</sup>, Miranda Thomas<sup>4</sup>,  
5 Lawrence Banks<sup>4</sup>, Vjekoslav Tomaić<sup>1#</sup>

6

7 1 Division of Molecular Medicine, Ruđer Bošković Institute, Bijenička cesta 54, 10000 Zagreb,  
8 Croatia

9 2 Division of Molecular Biology, Ruđer Bošković Institute, Bijenička cesta 54, 10000 Zagreb, Croatia

10 3 Institute of Virology, University of Cologne, Medical Faculty and University Hospital Cologne,  
11 Fürst-Pückler-Str. 56, 50935, Cologne, Germany

12 4 International Centre for Genetic Engineering and Biotechnology, AREA Science Park, Padriciano  
13 99, I-34149 Trieste, Italy

14

15 # Corresponding author: Vjekoslav Tomaić, tomaic@irb.hr

16 \* These authors contributed equally to this work.

17 Short title: HPV E6 oncoprotein stability is MAML1 dependent

18 Keywords: HPV, E6, cervical cancer, skin cancer, E6AP, MAML1, proliferation, migration,  
19 oncogenesis

20           **Abstract**

21           While a small proportion of high-risk (HR) alpha ( $\alpha$ ) Human Papillomaviruses (HPVs) is associated  
22 with numerous human malignancies, of which cervical cancer is the most prevalent, beta ( $\beta$ ) HPVs  
23 predominantly act as co-factors in skin carcinogenesis. A characteristic feature of both  $\alpha$ - and  $\beta$ -E6  
24 oncoproteins is the presence of the LXXLL binding motif, which  $\alpha$ -E6s utilize to form a complex with E6AP  
25 and which enables  $\beta$ -E6s to interact with MAML1. Here we show that multiple  $\alpha$ -E6 oncoproteins bind to  
26 MAML1 via the LXXLL binding motif and that this results in increased protein stability. Moreover,  $\beta$ -E6  
27 oncoprotein stability is also dependent on the interaction with MAML1. Additionally, in the absence of  
28 MAML1, endogenous HPV-8 E6 and HPV-18 E6 are rapidly degraded at the proteasome. Ablation of both  
29 E6AP and MAML1 leads to an even more profound down-regulation of  $\alpha$ -E6 protein expression, whereas  
30 this is not observed with  $\beta$ -E6. This highly suggests that there is one cellular pool for most of  $\beta$ -E6 that  
31 interacts solely with MAML1, whereas there are two cellular pools of HR  $\alpha$ -E6, one forming a complex with  
32 MAML1 and the other interacting with E6AP. Furthermore, MAML1 induces HPV-8 E6 shuttling from the  
33 nucleus to the cytosolic fraction, while MAML1 interaction with HR E6 induces a drastic nuclear and  
34 membrane upregulation of E6. Interestingly, the HR  $\alpha$ -E6 /MAML1 complex does not affect targeting of  
35 some of the known HR E6 cellular substrates such as p53 and DLG1. However, MAML1 and E6AP joint co-  
36 expression with HR  $\alpha$ -E6 leads to a significant increase in cellular proliferation, whereas silencing MAML1  
37 decreases wound closure in HeLa cells. These results demonstrate that HR  $\alpha$ -E6 interaction with MAML1  
38 results in a stable form of E6, which likely modulates MAML1's normal cellular activities, one consequence  
39 of which being an increased proliferative capacity of HPV-transformed cancer cells. Thus, this study shows  
40 a novel function of the  $\alpha$ -E6 oncoprotein and how it's activity might affect HPV-induced pathogenesis.

41

## 42 Introduction

43 Human papillomaviruses (HPVs) are a family of small DNA viruses that infect epithelial cells at  
44 various anatomical sites of the human body. It is a large and diverse group of viruses, divided into five  
45 genera (alpha ( $\alpha$ ), beta ( $\beta$ ), gamma ( $\gamma$ ), mu ( $\mu$ ) and nu( $\nu$ )) based on the open reading frame sequences  
46 coding for the L1 capsid protein. Thus far, more than 200 different HPVs have been discovered and  
47 recognized by the International Human Papillomavirus Reference Center [1]. Of the five genera,  $\alpha$  and  $\beta$   
48 have been most extensively studied, mostly due to their ability to cause pathological conditions in humans.  
49 Based on their ability to promote carcinogenesis,  $\alpha$ -HPVs can be classified as either high-risk (HR) or low-  
50 risk (LR), with no such classification existing for  $\beta$ -HPVs [1].

51 Almost all HPV types classified as cancer-causing reside within the genus  $\alpha$ -papillomavirus. Cancers  
52 caused by these types are predominantly anogenital, the most important of which being cervical cancer,  
53 but also include a subset of head and neck cancers [1,2]. Of all HR HPVs, HPV-16 and HPV-18 account for  
54 the vast majority of HPV-associated malignancies –approximately 70% world-wide cervical cancer cases,  
55 with the remaining 30% being caused by other HR HPVs [3]. By contrast, infections with LR  $\alpha$ -HPV types ,  
56 such as HPV-6 and HPV-11, merely lead to self-limiting benign warts [1,4]. The oncogenic potential of HR  
57 HPVs is attributed to the E6 and E7 oncoproteins and their interaction with a diverse range of cellular  
58 substrates, the most pivotal of which being p53 and pRB, respectively [5,6]. The E7 oncoprotein binds to  
59 pRB as well as other members of the pocket protein family and targets them for destruction by the  
60 ubiquitin-proteasome system [7]. Thus, E7 effectively disables the G1 cell cycle checkpoint, promotes cell  
61 proliferation and, as an unintended consequence, contributes to genomic instability [8]. HPV E6 forms a  
62 tertiary complex with the E6AP (E6-associated protein) ubiquitin ligase and p53, which leads to p53  
63 polyubiquitination and degradation by the proteasome, ensuring the resistance of infected cells to  
64 apoptosis, and cell cycle progression [9,10]. Furthermore, analyses of the association between E6 and E6AP  
65 have revealed that the protein stability of HR E6 oncoproteins was dependent on the presence of E6AP.

66 Moreover, ablation of E6AP from HPV-18 positive HeLa cells resulted in a dramatic increase in E6  
67 oncoprotein turnover at the proteasome [11]. In addition to p53, HR E6 oncoproteins also target a number  
68 of other cellular substrates for a proteasomal degradation in both E6AP-dependent and -independent  
69 manners, resulting in the modulation of various cellular pathways. Some of the more comprehensively  
70 described E6 targets include DLG1, SCRIB and the MAGI protein family members, which are all PDZ domain-  
71 containing proteins involved in several important cellular processes ranging from cell growth, polarity and  
72 adhesion to cell differentiation, proliferation, apoptosis, migration and intracellular trafficking [12,13].

73 Unlike  $\alpha$ -HPVs, HPVs of the genus  $\beta$  are not considered carcinogenic by themselves, but can  
74 contribute to the development of skin cancer in the presence of certain underlying health conditions, such  
75 as in patients with the genetic disorder Epidermodysplasia verruciformis (EV) or in otherwise  
76 immunocompromised individuals [14,15].  $\beta$ -HPV types, such as HPV-5 and HPV-8, have been found in EV  
77 patient skin lesions and squamous cell carcinoma samples, however, subsequent analyses have shown that  
78  $\beta$ -HPVs do not cause the cancer but facilitate carcinogenesis by inhibiting apoptosis in response to UV  
79 damage [16]. Like their  $\alpha$ -HPV counterparts,  $\beta$ -HPVs also employ E6 and E7 proteins, yet with some  
80 significant differences. For instance, while  $\beta$ -E7s bind to pRB tumor suppressor, they do so with much  
81 weaker affinity than  $\alpha$ -E7s, and thus this binding does not induce pRB degradation. Unlike  $\alpha$ -HPV E6  $\beta$ -E6  
82 oncoproteins do not target p53 for proteasome-mediated degradation, but inhibit its stabilization in  
83 response to genome-destabilizing events, thus allowing for the accumulation of DNA damage [17]. Of note,  
84 the  $\beta$ -genus HPV-38 E7 oncoprotein additionally stabilizes p53 [8,18]. Interestingly, a recent study has  
85 demonstrated that, while  $\alpha$ -E6s form a complex with E6AP and thus modulate its ubiquitin ligase activity,  
86 E6 oncoproteins of the other four genera, including  $\beta$ -E6s, preferentially bind MAML1 (Mastermind Like  
87 Transcriptional Coactivator 1) [19]. Nevertheless, it is important to note that, while a distinction between  
88 the preferred binding partners of different genera exists, this binding preference is by no means mutually

89 exclusive, as some cutaneous HPV E6s have been shown to also interact with E6AP, which contributes to  
90 E6 protein stabilization [20].

91 MAML1 is a transcriptional co-activator of the Notch signaling pathway. Activated Notch signaling  
92 has different effects depending on different cells and tissue types, and this complexity is notably profound  
93 in the context of HPV infection, where Notch activation has been found to be both positively and negatively  
94 involved in HR HPV infection and progression of infected tissues from precursor lesions towards cervical  
95 cancers [21]. During HPV infections of cutaneous epithelia  $\beta$ -HPV E6 oncoproteins interact with MAML1 to  
96 prevent the formation of the Notch-activating complex and, thus preventing differentiation and cell cycle  
97 arrest, and in this way enabling the viruses' survival and stability in skin keratinocytes [22]. It is currently a  
98 well-established fact that the binding of  $\alpha$ -E6s to the LXXLL motif on E6AP is crucial for their interaction and  
99 for the subsequent cellular functions of these E6 oncoproteins [11,23,24].  $\beta$ -E6 and MAML1 interact via  
100 the same binding motif present on both proteins, and the effects of these interactions on the Notch  
101 signaling pathway have been characterized in numerous reports as well. However, to the best of our  
102 knowledge, no detailed research has been done on investigating the effects of MAML1 binding on E6  
103 protein stability and how this might affect E6 functionality [25–27]. Therefore, we wanted to investigate  
104 whether the binding of both  $\alpha$ - and  $\beta$ -HPV E6 to MAML1 would have an effect on E6 oncoprotein stability  
105 and, if so, how this might influence E6 molecular activities and their potential impact on cell proliferation  
106 and migration.

107 In the present manuscript, we show that MAML1 binding to E6 leads to increased protein stability,  
108 not only in the case of  $\beta$ -E6s, but also for E6 proteins of the genus  $\alpha$ . MAML1 binds to a defined cellular  
109 pool of HR E6 oncoproteins, but does not influence its capacity to target tumor suppressors p53 and DLG1  
110 for proteasome-mediated degradation. However, MAML1 decreases the rate of protein turnover of this  
111 distinct pool of HR E6 oncoprotein as well as of HPV-8 E6 oncoprotein, and this appears to be E6AP-

112 independent. Furthermore, E6AP and MAML1 increase cellular proliferation by synergistically stabilizing HR  
113 E6 protein levels, which is likely to have a profound role on HPV-driven oncogenesis.

## 114 **Materials and methods**

### 115 *Cell lines and culture, transfections*

116 HEK-293 (human embryonic kidney), CRISPR/Cas9 gRNA-mediated E6AP-null HEK-293 cells [24] ,  
117 HeLa (cervical carcinoma, HPV-18 positive), CaSki (cervical carcinoma, HPV-16 positive), HT1080 8 E6  
118 (fibrosarcoma epithelial cells, stably expressing HPV-8 E6) [17] and C33A (cervical carcinoma, HPV-negative)  
119 cells were used in the experiments. All cell lines were grown in Dulbecco's modified Eagle's medium  
120 (DMEM) (Gibco, Thermo Fisher Scientific, USA) with 10% fetal bovine serum (FBS) (Gibco, Thermo Fisher  
121 Scientific, USA) and penicillin/streptomycin (100 U ml<sup>-1</sup>) (Gibco, Thermo Fisher Scientific, USA) and L-  
122 glutamine (300 µg ml<sup>-1</sup>) (Gibco, Thermo Fisher Scientific, USA) at 37°C in a humidified air incubator  
123 containing 10 % CO<sub>2</sub>. Cells were transfected by calcium phosphate precipitation method [28] and analyzed  
124 or harvested 24hrs or 48hrs post transfection. Cells transfected with β-galactosidase and a suitable amount  
125 of empty pcDNA3 vector were used as controls for transfection efficiency.

### 126 *Plasmids*

127 HA-tagged HPV-8, -11, -12, -14, -16, -18, -24, -33 and -38 E6, as well as pcDNA3 FLAG-E6AP,  
128 pcDNA3-FLAG-p53 [20,29,30] and pcDNA3 plasmid expressing HA-DLG1, cloned into pcDNA3 expression  
129 vectors were used and have been described previously [31]. Other plasmids included a FLAG-tagged  
130 MAML1 cloned into pCMV2-FLAG plasmid, pCMV2-FLAG MAML LHHLL mutant [32], pCS2 MYC-MAML1  
131 [33], pCIG-MYC E6AP [34], the empty vector pXJ41-FLAG or pXJ41-16E6-FLAG coding for FLAG-tagged  
132 HPV16 E6 [35]. pGEX-2T:16E6, pGEX-2T:18E6, pGEX-2T:E6 and pGEX-2T:11E6 plasmids expressing the GST-  
133 E6 fusion proteins have been previously described [11,30,36].

134            *Antibodies*

135            The following antibodies were used: anti-MAML1 (clones D3E9 and D3K7B) (Cell Signaling  
136            Technology, USA), anti-E6AP (UBE3A; clone 13/UBE3A) (BD Bioscience, USA), anti-p53 (clone DO-1) (Santa  
137            Cruz Biotechnology, USA), anti- $\beta$ -actin-HRP (clone B-7) (Sigma-Aldrich, DE), anti-HPV-18 E6 (clone G-7)  
138            (Santa Cruz Biotechnology, USA), anti-HA-peroxidase (clone HA-7) (Sigma-Aldrich, DE), anti-FLAG (clone  
139            M5, Sigma-Aldrich, DE), anti-FLAG (H-5) (Santa Cruz Biotechnology, USA), anti-c-myc (9E10) (Santa Cruz  
140            Biotechnology, USA), anti- $\beta$ -galactosidase (Promega, USA), anti-DLG1 (SAP-97, clone 2D11) (Santa Cruz  
141            Biotechnology, USA), anti-MCM7 antibody (clone 141.2) (Santa Cruz Biotechnology, USA), anti-GAPDH  
142            antibody (Abcam, UK), anti-histone H3 antibody (clone D1H2) (Cell Signaling Technology, USA) and anti-  
143            Vimentin antibody (clone E5) (Santa Cruz Biotechnology, USA), GAPDH-Alexa Fluor 680 (G9, Santa Cruz  
144            Biotechnology, USA); and mouse and rabbit secondary antibodies conjugated to horseradish peroxidase  
145            (HRP) (Dako, Agilent, USA), IRDye-coupled secondary antibody and rhodamine red or Alexa Fluor 488  
146            (Invitrogen, Thermo Fisher Scientific, USA).

147            *Inhibitors*

148            The inhibitors were dissolved in dimethyl sulfoxide (DMSO) and used at the indicated  
149            concentrations. The proteasome inhibitor bortezomib (BTZ; 10  $\mu$ M) (Sigma-Aldrich, DE) was used at the  
150            concentration 1:10000. Cycloheximide (Sigma-Aldrich, DE) was used at the concentration 1:1000 in order  
151            to block protein synthesis in half-life experiments. The lysis buffers were supplemented with protease  
152            inhibitor, 1  $\times$  Cocktail Protease Inhibitors (Roche Diagnostics, DE).

153            *Western blot*

154            Following treatment, cells were harvested by scraping, centrifuged and pellets resuspended in SDS  
155            buffer (100 mM Tris HCl pH=6,8, 200 mM DTT, 4% SDS, 20% glycerol and bromophenol blue). Samples were  
156            then subjected to sonification (1'') and heated at 95°C for 10'. Proteins were separated on either 7,5% or

157 10% sodium dodecyl sulfate - polyacrylamide gels (SDS-PAGE) and transferred by tank blotting to a  
158 nitrocellulose membrane with a pore size of 0,2  $\mu\text{m}$ . Membranes were blocked with 10% dry milk in PBS or  
159 TBS containing 0,1% Tween-20 (PBST/TBST) for 30' at 37°C, after which they were incubated with indicated  
160 antibodies diluted in 10% milk in PBST or TBST (2h at RT or overnight at 4°C). Membranes were washed in  
161 PBST or TBST (3 x 10') and then incubated for 1h with HRP-linked secondary antibodies (anti-rabbit 1:1000  
162 or anti-mouse 1:1000), after which they were washed again. Signals were developed either with  
163 SuperSignal™ West Pico PLUS Chemiluminiscent Substrate (Thermo Fisher Scientific, USA) or Amersham  
164 ECL western blotting detection reagents (Cytiva, USA) detected by Uvitec Cambridge – Alliance 4.7 and  
165 Alliance Q9 imaging systems (Cleaver Scientific, UK) or a LI-COR Odyssey Fc imager (LI-COR, USA), and  
166 quantified by ImageJ [37]. If needed, antibodies were detached from membrane using with 0.2 M NaOH  
167 for 20' after which membranes were re-probed. E6 band intensity was first normalized with the image  
168 background after which it was divided with that of normalized  $\beta$  galactosidase (LacZ) which served as  
169 transfection control. The average normalized relative expression of E6 of at least four experiments where  
170 E6 was transfected alone, was taken as control. All the normalized relative expressions of E6 (transfected  
171 alone or with MAML1 or E6AP) were expressed as fold changes in regards to the control E6. The LOG2 of  
172 these fold changes was calculated to better depict the increase or decrease in protein amounts. The same  
173 procedure was applied in experiments with p53 and DLG1 overexpression.

#### 174 *Immunoprecipitation*

175 HEK-239 cells were transfected with an empty plasmid, HA-tagged HPV-16 E6 and HPV-8 E6 alone,  
176 or in combination with FLAG-MAML1, FLAG-MAML1 (LHHLL) or myc-MAML1 (LHHLL). For  
177 immunoprecipitation experiments, transfected cells were harvested by scraping and centrifuged. Cell  
178 pellets were resuspended on ice in modified E1A lysis buffer (0.25% NP-40, 1 mM EDTA, 50 mM HEPES, pH  
179 7.4, 150 mM NaCl). Samples were subjected to sonification (2 x 30'') and left on ice for 20'. After  
180 centrifugation supernatants were collected and incubated with anti-HA beads (Sigma-Aldrich, DE) for 2hrs

181 on a rotating wheel at RT. The beads were extensively washed and subjected to western blot analysis with  
182 anti-FLAG or anti-myc antibodies. C33A cells were transfected with the empty vector pXJ41-FLAG or pXJ41-  
183 16E6-FLAG coding for FLAG-tagged HPV16 E6. Cell extracts were generated 48hrs post transfection using  
184 low salt dilution buffer (LSDB) (50 mM Tris/HCl (pH 8), 20 % Glycerol, 100 mM KCl, 0,1% NP40, 1 mM DTT,  
185 50 mM NaF, 1 mM orthovanadate, 1 mM PMSF), followed by incubation with anti-FLAG antibody coupled  
186 to magnetic beads (Thermo Fisher Scientific, USA) for 2hrs at room temperature, followed by three washes  
187 with LSDB. Co-precipitated cellular proteins were detected by western blotting with anti-MAML1 and anti-  
188 FLAG.

#### 189 *Fusion protein purification and GST pull-down assay*

190 DH5 $\alpha$  *Escherichia coli* competent cells were transformed with GST-E6 constructs (GST-16 E6, -18  
191 E6, -11 E6 and -8 E6) and GST fusion protein synthesis and protein purification were performed as  
192 previously described [38]. GST- pull-down assays using cellular extracts were performed by incubating equal  
193 amounts of GST-tagged proteins immobilized on glutathione agarose, with pre-cleared whole cell lysates  
194 of HEK-293 cells (previously transfected with FLAG-tagged MAML1) in modified E1A buffer (0.25% NP-40,  
195 1 mM EDTA, 50 mM HEPES, pH 7.4, 150 mM NaCl) for 2hrs on a rotating wheel at 4°C. After extensive  
196 washing with E1A buffer, the bound proteins were detected using SDS-PAGE and western blotting with  
197 anti-FLAG antibody.

#### 198 *siRNA silencing*

199 The cells were seeded on 60 mm tissue culture dishes and transfected the following day with ON-  
200 TARGETplus human MAML1 siRNA (siMAML1, smartpool, Horizon discovery, UK) and ON-TARGETplus  
201 human UBE3A siRNA (siE6AP, individual, Horizon discovery, UK) according to the manufacturer's  
202 instructions and harvested 72hrs after silencing. siRNA against luciferase (siLuc, individual, Horizon  
203 discovery, UK) was used as control.

204 *Immunofluorescence*

205 HeLa and HT1080 8 E6 cells were grown overnight on coverslips and transfected the following day.  
206 Seventy-two hrs post transfection cells were fixed with 4.7% paraformaldehyde for 10' at RT and  
207 permeabilized in PBS containing 0.1% Triton X-100. The staining was performed by incubating samples with  
208 indicated antibodies diluted in PBS overnight at 4°C in a humidified chamber. After washing, the coverslips  
209 were incubated with fluorescently conjugated mouse or rabbit secondary antibodies. Nuclei were labelled  
210 with DAPI [36]. Samples were monitored on a laser scanning microscope Leica TCS SP8 X, equipped with a  
211 HC PL APO CS2 63×/1.40 oil objective (Leica Microsystems, DE).

212 *Half-life experiments*

213 HeLa cells and HT1080 HPV-8 E6 expressing cells were transfected with siRNA against luciferase  
214 (siLuc – control), siMAML1 and siE6AP alone or in combination. Seventy-two hrs later, prior to harvesting,  
215 cells were treated with cycloheximide (Sigma-Aldrich, DE), which was added in fresh medium. The cells  
216 were harvested at time points indicated and analyzed by western blotting. siRNA against luciferase was  
217 used as control.

218 *Cell fractionation assays*

219 For cell fractionation analyses, HEK-293 cells were seeded on 100 mm tissue culture dishes at a  
220 density of approximately  $7 \times 10^5$  prior to transfections. Twenty-four hrs post transfection the cells were  
221 collected by scraping and fractionated into cytoplasmic, membrane, nuclear and cytoskeletal fractions  
222 using the ProteoExtract Cell Fractionation Kit (Calbiochem, Merck, USA) according to the manufacturer's  
223 instructions. The fractions were analyzed by SDS-PAGE followed by western Blotting using anti-HA antibody  
224 (Sigma-Aldrich, DE), anti-MCM7 antibody (clone 141.2) (Santa Cruz Biotechnology, USA), anti-GAPDH  
225 antibody (Abcam, UK), anti-histone H3 antibody (clone D1H2) (Cell Signaling Technology, USA) and anti-  
226 Vimentin antibody (clone E5) (Santa Cruz Biotechnology, USA) as indicated.

227 *Cell proliferation assay*

228 The assay was performed as described previously [39]. In brief, HEK-293 cells ( $1.2 \times 10^5$ ) were  
229 seeded on 60 mm tissue culture dishes, cultured overnight and transfected by calcium phosphate  
230 precipitation method [28], using a total of 9.0  $\mu\text{g}$  of plasmid DNA. The cells were transfected with pcDNA3  
231 plasmids expressing HPV-16 E6 and HPV-8 E6, alone or in combination with MAML1, E6AP or both as  
232 indicated. In order to monitor transfection efficiency, cells were co-transfected with  $\beta$ -galactosidase (LacZ)  
233 and verified by western blotting using the appropriate antibodies. Twenty-four hrs post transfection, the  
234 cells were detached, counted, and seeded at  $0.5 \times 10^4$  cells per well to a final volume of 100  $\mu\text{l}$  in a 96-well  
235 plate and incubated for a further 48hrs. Cell proliferation was monitored using Uptibblue reagent (Interchim)  
236 as previously described [39]. Uptibblue reagent (5% [vol/vol]) was added to the culture medium 72hrs after  
237 transfection, and absorbance was measured at 575 nm and 590 nm on a Labystems Multiskan MS 352  
238 multiwell plate reader with accompanying Ascent Software (Thermo Fischer Scientific, USA). The results are  
239 expressed as a percentage of the reduced Uptibblue reagent with the indicated standard error of the mean  
240 (SEM).

241 *Wound healing/scratch assay*

242 A monolayer scratch/wound healing assay was done as described previously [40]. HeLa and HT1080  
243 8 E6 cells were transfected with a control siLuc, siMAML1 and siE6AP as indicated. After 48hrs, a scratch  
244 wound was generated in the confluent cells with a sterile Artline p2 pipette tip (Thermo Fisher Scientific,  
245 USA). The wounds were photographed under a microscope using a Dino-Eye digital eyepiece camera  
246 (AM7023(R4); IDCP B.V., NE) that was connected to a computer and DinoCapture 2.0 microscope imaging  
247 software. After an additional 24hrs, the wounds were photographed again, and wound closure was  
248 calculated; the images were saved in TIFF format, and gap areas were measured using the MRI wound  
249 healing tool macro for ImageJ software (NIH)[37] ([http://dev.mri.cnrs.fr/projects/imagej-](http://dev.mri.cnrs.fr/projects/imagej-macros/wiki/Wound_Healing_Tool)  
250 [macros/wiki/Wound\\_Healing\\_Tool](http://dev.mri.cnrs.fr/projects/imagej-macros/wiki/Wound_Healing_Tool)). The cells were then harvested by scraping, centrifuged and pellets

251 resuspended in SDS buffer. MAML1, E6AP and E6 protein levels were analyzed by western blotting.  $\beta$ -actin  
252 was used as a loading control.

### 253 *Statistical analysis*

254 Data were analyzed by GraphPad Prism (GraphPad Inc. USA). The differences and their statistical  
255 significance between groups were determined by one-way ANOVA or student's t-test. P values of under  
256 0.05 were considered significant (\*), under 0.01 very significant (\*\*) and under 0.001 extremely statistically  
257 significant (\*\*\*). All values are averages of at least three independent experiments and the standard error  
258 of the mean is depicted as error bars.

## 259 **Results**

### 260 *HPV E6 oncoproteins from $\alpha$ and $\beta$ types interact with MAML1*

261 Several proteomic analyses have demonstrated an interaction between a number of  $\beta$ -HPV E6  
262 oncoproteins and MAML1, a co-activator of the Notch signaling pathway [25,26]. One of these studies also  
263 showed an association between MAML1 and HPV-16 E6 in co-immunoprecipitation assays, although the  
264 association described there was only minimal [25]. To verify that MAML1 is indeed a binding partner of  
265 both  $\alpha$ - and  $\beta$ -HPV E6 oncoproteins we first performed co-immunoprecipitation analyses using HEK-293  
266 cells, which had been transfected with either an empty plasmid, or plasmids expressing HA-tagged HPV-16  
267 E6 and HPV-8 E6, alone or in combination with FLAG-tagged MAML1. Twenty-four hrs post transfection the  
268 cells were harvested and lysed, and the cell extracts were incubated with anti-HA beads. The protein  
269 complexes immunoprecipitated in this manner were analyzed by western blot. The results shown in Figure  
270 1A demonstrate an interaction between HPV-8 E6 and MAML1, as well as a somewhat weaker, but still very  
271 evident interaction between HPV-16 E6 and MAML1. To additionally verify these observations, we  
272 expanded our analysis and conducted co-immunoprecipitation assays between ectopically expressed 16 E6  
273 and endogenous MAML1 in the HPV-negative cervical tumor derived cell line C33A. The cells were

274 transfected either with an empty plasmid or plasmid expressing FLAG-tagged 16 E6. Cell extracts were  
275 generated 48hrs post transfection, incubated with anti-FLAG-antibody coupled to magnetic beads and the  
276 immunoprecipitated complexes were further subjected to western blot analysis. As indicated in Figure 1B,  
277 16 E6 also interacted with endogenous MAML1 in this experimental setting, further supporting the  
278 observation that these two proteins form a complex. These results corroborate those previously published,  
279 which state that, even though there is a distinct preference across different  $\beta$ -HPV types for MAML1, HPV  
280 genera cannot be exclusively divided based on this interaction [19]. Next, we were interested in  
281 investigating whether MAML1 could complex with other  $\alpha$ -type E6 oncoproteins. To establish this, we  
282 performed a series of glutathione S-transferase (GST) pull-down assays using GST-16 E6, GST-18 E6, GST-  
283 11 E6, GST-8 E6 fusion proteins, or GST alone as a control. Bound proteins were detected by SDS-PAGE and  
284 western blotting, and the results are shown in Figure 1B. In this setting, we observed that E6 proteins from  
285 all the HPV types tested bind to MAML1. HPV-8 E6 interaction was decisively the strongest, followed by 18  
286 E6, with a weaker interaction with 16 E6, while the interaction with 11 E6 was the weakest (Figure 1B).  
287 Taken together these results suggest that, even though E6 oncoproteins from  $\alpha$ - and  $\beta$ -HPV types can  
288 complex with MAML1, the preferred interacting partners are E6 oncoproteins from the  $\beta$  genus.

### 289 *MAML1 stabilizes E6 oncoproteins from $\alpha$ - and $\beta$ -HPV types*

290 After confirming that both  $\alpha$ - and  $\beta$ -HPVs interact with MAML1, we sought to establish whether  
291 these interactions have any impact on E6 oncoprotein stability. HEK-293 cells were transfected with a panel  
292 of plasmids expressing HA-tagged E6 proteins from HPV types -8, -12, -14, -16, -18, -24, -33 and -38, either  
293 alone or in combination with FLAG- or Myc-tagged MAML1 or E6AP. After overnight incubation, the  
294 transfected cells were harvested and proteins isolated, separated and analyzed by means of western  
295 blotting. E6 protein band intensities from HEK-293 cells transfected with the panel of E6s alone were  
296 compared with those co-transfected with MAML1 or E6AP. Considering that the stabilizing effect of E6AP  
297 on HR HPV E6 oncoproteins is well defined [11], we chose to compare the impact of MAML1 on E6 stability

298 with that of E6AP. As shown in Figure 2A (Supplementary Figure 1, left panel), E6 oncoproteins of all HPV  
299  $\alpha$ - and  $\beta$ -types analyzed were stabilized by MAML1, showing that HPV proteins cannot be separated based  
300 on MAML1 and E6AP association, as well as demonstrating a previously unknown role for MAML1 in E6  
301 stabilization. As expected, E6AP stabilized  $\alpha$ -type HPV E6s, but, interestingly, also  $\beta$ -types 24 E6 and 38 E6,  
302 which were previously reported to bind E6AP [20].

303 As HEK-293 cells endogenously express the functional E6AP ubiquitin ligase, it was necessary to  
304 confirm that the upregulation of E6 observed in HEK-293 cells was MAML1 specific and not dependent on  
305 the effects of the endogenous E6AP. For this reason, HEK-293 E6AP knock-out cells (E6AP KO) [24] were  
306 transfected with plasmids expressing HA-tagged E6 proteins from HPV types -8, -12, -14, -16, -18, -24, -33  
307 and -38 E6, either alone or together with MAML1 or E6AP, and analyzed in the manner described above.  
308 E6 proteins of all HPV types tested were again stabilized by MAML1 (Figure 2B and Supplementary Figure  
309 1, right panel), supporting the initial observations and confirming that the stabilizing effect is indeed due  
310 to MAML1, and is independent of E6AP. Transfecting E6AP KO cells with plasmid expressing HPV-24 E6,  
311 alone or in combination, again provided the same results, as did the transfection with plasmid expressing  
312 HPV-38 E6 protein, confirming the observation that both MAML1 and E6AP stabilize those cutaneous types.  
313 Interestingly, whilst E6 protein stabilization by E6AP and MAML1 was evident in both cellular backgrounds,  
314 the actual degree of stabilization varied among different E6 types examined. This is likely to be attributed  
315 to the differences in strength of the interactions between MAML1 and E6 proteins among distinct HPV  
316 types, as evident from the GST pull-down assays.

### 317 *E6 protein stabilization is LXXLL dependent*

318 Both MAML1 and E6AP share a common structural feature - the LXXLL motif, through which they  
319 interact with E6 oncoproteins.  $\alpha$ -HPV E6 oncoproteins associate with E6AP by binding to a conserved LXXLL  
320 motif on E6AP, forming a stable complex which targets a number of cellular substrates for proteasome-

321 mediated degradation [9,41]. This interaction is also responsible for E6 oncoprotein stability, which is  
322 further reflected by the effects E6 has on global transcription [11,23]. The C-terminus of MAML1 carries an  
323 acidic domain containing the LXXLL motif responsible for interacting with  $\beta$ -HPV E6 [25,26]. Therefore, we  
324 aimed at further elucidating whether an intact, wild type LDDLL motif might be necessary for MAML1 to  
325 form a complex with E6 and consequently induce E6 protein stabilization. In order to investigate this, we  
326 transfected HEK-293 cells with plasmids expressing HPV-16, -18, and -8 E6 oncoproteins either alone or  
327 together with a wild type MAML1 or a MAML1 mutant (MAML1 LHHLL). The mutant in this experiment had  
328 the two aspartate residues of the LDDLL motif, which have previously been described to be indispensable  
329 for the interaction, mutated to histidines (LHHLL) [32]. Regardless of the mutated LDDLL domain, we  
330 observed that both  $\alpha$ - and  $\beta$ -HPV E6 oncoproteins were again stabilized. HPV -8 and -18 E6s were stabilized  
331 by both wt MAML1 and the mutant, but the mutant stabilized E6 to a lesser degree than the wt MAML1  
332 (Figure 3A, top panel and Supplementary Figure 2A, left panel). Interestingly, HPV-16 E6 was not stabilized  
333 by the MAML1 mutant, possibly because its initial interaction was weaker and thus completely abrogated  
334 by mutating the residues (Figure 3A, top panel). Again, the findings were confirmed by repeating the same  
335 experiment in HEK-293 E6AP KO cells, resulting in the same effect on E6 oncoproteins (Figure 3A bottom  
336 panel and Supplementary Figure 2A, right panel). We sought to further explore these findings by  
337 performing co-immunoprecipitation experiments of HPV-8 E6 oncoproteins with wt and mutated MAML1.  
338 Here we found that, indeed, the mutation did not fully abrogate the interaction (Figure 3B and  
339 Supplementary Figure 2B). Therefore, it is likely that all 5 amino acids or even other amino acids upstream  
340 or downstream of the LXXLL motif are involved in the association with E6s, since the mutant still interacted  
341 with HPV-8 E6, although to a lesser extent, which was then reflected by a reduction of E6 protein  
342 stabilization.

343            *HPV E6 protein stability in CaSki, HeLa and 8 E6 expressing HT1080 cells is MAML1-*  
344 *dependent*

345            Having established that ectopic co-expression of MAML1 and E6 oncoproteins from  $\alpha$ - and  $\beta$ -HPV  
346 types leads to stabilization of E6 protein levels in HEK-293 cells and HEK-293 E6AP KO cells, we wanted to  
347 further examine this effect in HPV-positive cell lines, which endogenously express E6. In order to achieve  
348 our goal we used cervical cancer-derived HeLa cells, which contain HPV-18 E6/E7 DNA sequences; CaSki  
349 cells, which contain HPV-16 E6/E7 DNA sequences; and HT1080 cells, stably expressing FLAG-tagged HPV-  
350 8 E6 [17]. To assess whether the stabilization indeed occurs at the protein level, MAML1 and E6AP were  
351 silenced in these cell lines by transfection with appropriate siRNAs, while the proteasome activity was  
352 abrogated using the proteasomal inhibitor Bortezomib (BTZ). The effects of silencing on the E6 oncoprotein  
353 expression in HeLa and HPV-8 E6 expressing HT1080 cells were assessed using primary antibodies, with the  
354 effect on the E6 protein levels in CaSki cells being extrapolated from the p53 levels, as multiple previous  
355 studies had confirmed that p53 is degraded in the presence of HR E6 and cellular E6AP [6,9,42].

356            Silencing MAML1 in HeLa cells induced a notable decline in HPV-18 E6 protein levels, with inhibition  
357 of proteasomal degradation nullifying this effect, which demonstrates that this process is proteasome-  
358 dependent. Interestingly, silencing MAML1 had no effect on p53 protein levels, even though it would have  
359 been expected that a decrease in the amount of E6 would also result in a reduction of p53 degradation  
360 (Figure 4A) [9,43]. However, this effect was observed when E6 was downregulated as a result of E6AP  
361 silencing, which is consistent with previously published results (Figure 4A) [11]. When the same experiment  
362 was performed in CaSki cells, the expression profile of p53 was similar to the one observed in HeLa cells.  
363 Silencing E6AP resulted in the depletion of E6 and subsequent accumulation of p53 (Figure 4B).  
364 Furthermore, silencing MAML1 in HPV-8 E6 expressing HT1080 cells also resulted in downregulation of E6.  
365 This effect was nullified when BTZ was added, suggesting that MAML1 also stabilizes HPV-8 E6 in a  
366 proteasome-dependent manner (Figure 4C). Conversely, silencing E6AP had no discernable effect on HPV-

367 8 E6 levels (Figure 4C). These results are in accordance with those depicted in Figure 2, where  
368 overexpression of E6AP with HPV-8 E6 does not lead to its increased protein stabilization. Even though  
369 E6AP has been shown to interact with some E6 oncoproteins of  $\beta$ -HPV types and stabilize them, no such  
370 studies, thus far, have been performed for HPV-8 E6 [20].

371         Having established via western blot that MAML1 has an impact on HPV-16, -18 and -8 E6 protein  
372 stability, we aimed to further confirm these results by investigating how MAML1 knockdown influences  
373 cellular localization of HPV-18 and -8 E6 cellular pools. To assess this, we again performed siRNA silencing  
374 of E6AP and MAML1 in HeLa cells and HPV-8 E6-expressing HT1080 cells. Seventy-two hrs post transfection,  
375 cells were fixed and immunolabeled, and the localizations of both HPV-8 E6 and p53 (serving as a control  
376 for E6 expression in HeLa cells) proteins were monitored by laser confocal microscopy. As expected, E6AP  
377 ablation in HeLa cells led to p53 recovery in the nucleus, likely due to the downregulation of HPV-18 E6 in  
378 the absence of E6AP (Figure 5A). By contrast, there was no discernible effect on HPV-8 E6 protein levels  
379 under the same experimental conditions (Figure 5C). Ablation of MAML1 in HeLa cells did not have any  
380 effect on nuclear accumulation of p53 (Figure 5B), while MAML1 silencing in HPV-8 E6-expressing HT1080  
381 cells did result in the downregulation of nuclear HPV-8 E6 (Figure 5D). These results are in line with  
382 observations from our western blot analyses (Figure 4), suggesting that silencing MAML1 does not affect  
383 the HPV-18 E6 pool involved in p53 degradation. Furthermore, the fact that E6AP silencing did not have  
384 any effect on HPV-8 E6 protein stability additionally confirmed the aforementioned results (Figure 4C),  
385 indicating that there is likely only one pool of HPV-8 E6, which solely interacts with MAML1.

386         *p53 and DLG1 degradation is not E6/MAML1 complex dependent*

387         Following the observed effect on endogenous p53 in HPV-18 positive background, we sought to  
388 confirm the results by ectopically expressing the proteins in question in HEK293 E6AP KO cells. We wanted  
389 to see whether the opposite effect on p53 could be observed when overexpressing MAML1 or E6AP with

390 HPV-16 E6. As depicted in Figure 6A, MAML1 overexpression with HPV-16 E6 does not induce additional  
391 degradation of p53, even though it increases E6 protein levels. By contrast, overexpression of E6AP leads  
392 to both higher level of E6 and lower level of p53 (Figure 6A), as previously published [34].

393         Apart from p53, E6 targets a number of other cellular proteins for proteasome-mediated  
394 degradation and this process is considered to play an essential role in later stages of HPV-induced  
395 tumorigenesis. Some of these protein targets include PDZ domain-containing proteins, for example, the  
396 tumor suppressor DLG1 [41]. It was previously shown that catalytically active E6AP is essential for the ability  
397 of E6 to degrade p53, while DLG1 and the MAGI family proteins were shown to be degraded by E6 quite  
398 effectively without requiring E6AP, indicating that E6 targets these cellular substrates in an E6AP-  
399 independent manner [34]. Therefore, we proceeded by investigating whether MAML1 stabilization of HR  
400 E6 might have any impact on targeting DLG1. As with p53, we co-transfected HEK-293 E6AP KO cells with  
401 plasmids expressing DLG1 in the presence of HPV-16 E6, together with either wild type E6AP or MAML1.  
402 Twenty-four hrs later, the protein extracts were separated by electrophoresis and changes in DLG1 protein  
403 levels were assessed by immunoblotting. As can be seen in Figure 6B, DLG1 was degraded very effectively  
404 by HPV-16 E6 both in the absence and presence of the functional E6AP, as expected [34]. Ectopic co-  
405 expression of MAML1 and HPV-16 E6 did not result in any additional degradation of DLG1, when compared  
406 to 16 E6 alone. All of this suggests that the E6/MAML1 complex is likely to be involved in other cellular  
407 activities which do not involve degradation of some of the well-characterized E6 substrates. Taken together  
408 with our previous results, these observations suggest that, while both E6AP and MAML1 stabilize HPV-16  
409 and -18 E6, they do not promote stability of the same cellular pools of E6. When MAML1 is silenced, the  
410 remaining pool of E6 is still in complex with E6AP and retains its catalytic activities. However, when MAML1  
411 is overexpressed together with HR E6, the stability of the E6 pool bound to MAML1 is increased, yet it  
412 appears that this cellular pool of E6 is not catalytically active in targeting cellular proteins such as p53 or  
413 DLG1.

414 *HPV E6 protein turnover is regulated by MAML1*

415 Since we demonstrated that MAML1 silencing downregulates E6 steady state levels, we further  
416 wanted to examine the effects on E6 protein turnover. We again used siRNAs to silence MAML1, E6AP or  
417 both, in HeLa and HPV-8 E6-expressing HT1080 cells, also including siRNA against luciferase as a control.  
418 Seventy-two hrs post transfection protein synthesis was blocked by cycloheximide in order to determine  
419 the rate of E6 protein turnover under these conditions. After blocking protein synthesis, the cells were  
420 collected and proteins isolated at indicated time points, separated on SDS-PAGE and detected by western  
421 blot analysis. As previously reported, the half-life of HPV-18 E6 in control HeLa cells treated with siRNA  
422 luciferase was around 120' [11,44]. Silencing either MAML1 or E6AP led to a shorter E6 half-life; when  
423 MAML1 was ablated, the half-life of HPV-18 E6 was around 90', whereas silencing E6AP caused a shortening  
424 of half-life to around 80'. Simultaneous silencing of both MAML1 and E6AP induced a further decrease to  
425 approximately 60', demonstrating a synergistic effect on E6 half-life (Figure 7A). HPV-8 E6 stably expressed  
426 in HT1080 had a half-life longer than the 120' in this experimental setting. When MAML1 was silenced, the  
427 half-life decreased to between 90 and 120', while, as expected, silencing E6AP had no impact on HPV-8 E6  
428 half-life (Figure 7B). Silencing both MAML1 and E6AP did not lead to any further decrease of HPV-8 E6 half-  
429 life. These results further suggest that MAML1 has a direct role in HPV E6 protein turnover of both  $\alpha$ - and  
430  $\beta$ -HPVs. Additionally, the exclusive impact of MAML1 on HPV-8 E6 protein turnover regulation was further  
431 confirmed, as E6AP was again shown to have no direct impact on HPV-8 E6 stability.

432 *E6 cellular distribution is altered by MAML1*

433 Since both MAML1 and E6AP stabilize E6, we next aimed at determining whether these interactions  
434 may also influence subcellular distribution of E6. For this reason, we transfected HEK-293 cells with either  
435 HPV-16 or -8 E6, either alone or in combination with MAML1 or E6AP. Cellular proteins were extracted  
436 using the "ProteoExtract<sup>®</sup> Subcellular Proteome Extraction Kit" which allowed for further separation into  
437 cytosolic (C), membrane (M), nucleic (N) and microtubule (T) fractions. The fractionated proteins were

438 separated on SDS-PAGE and detected via western blotting. When transfected alone 16 E6 primarily  
439 localized in the cytosolic fraction. Co-transfection with E6AP led to a primary stabilization of cytosolic E6,  
440 but also to an increase in E6 in other fractions. When co-transfected with MAML1, these proportions  
441 changed, and there was a notable increase in the amounts of E6 detected in the nucleic and membrane  
442 fractions, which was also accompanied with MAML1 accumulation in these fractions (Figure 8). When  
443 examining the effect of MAML1 and E6AP on HPV-8 E6 localization, a different distribution of E6 was  
444 observed. E6AP had no discernible effects on HPV-8 E6 localization, while MAML1 caused an increase in  
445 the amount of E6 in the cytosol, where MAML1 was predominantly detected (Figure 8). The increase in the  
446 cytosolic E6, as well as the stabilization of the nucleic E6, further underpinned the immunofluorescence  
447 results (Figure 5D). Based on these results, as well as those from the gene silencing experiments (Figure 4),  
448 we further confirmed that MAML1 and E6AP have an impact on two distinct pools of HR HPV E6. This  
449 observation highly suggests that the proportion of E6 proteins stabilized by MAML1 likely has distinct  
450 cellular functions, and possibly different interacting partners compared with E6 stabilized by E6AP and, as  
451 a direct consequence of this, it may therefore be distributed in different cellular compartments.

#### 452 *E6/MAML1 complex impacts cell proliferation and migration*

453 Aforementioned experiments have shown that the ablation of MAML1 has a direct impact on the  
454 stability, distribution and turnover of E6. Thus, we wanted to assess whether these changes in E6 have an  
455 effect on the behavior of the cell, that is, whether the decrease in E6 levels leads to an alteration of the cell  
456 proliferation potential. To test this, we ectopically expressed HPV-18 or -16 E6, together with MAML1, E6AP  
457 or both, in HEK-293 E6AP KO cells. Five thousand transfected cells were transferred from dishes to 96 well  
458 plates in quadruplicates, and Uptiblue reagent was added in the log phase of growth to measure cell  
459 proliferation, 48hrs after the transfer. Absorbance was detected 5hrs later and the percentage of reagent  
460 reduction calculated. Compared with HPV-16 E6 transfected alone, transfection with E6AP led to an  
461 increase in the proliferation of E6AP KO cells, whereas transfection in combination with MAML1 did not

462 change the rate of proliferation. In cells co-transfected with all of the expression plasmids proliferation was  
463 significantly elevated, demonstrating a synergistic effect of MAML1 and E6AP (Figure 9). HPV-18 E6 showed  
464 a similar trend compared to that of HPV-16 E6. HPV-18 E6 alone induced an increase in cellular  
465 proliferation, which became even more pronounced with the addition of E6AP. Addition of both E6AP and  
466 MAML1 resulted in a further increase in proliferation, strongly hinting at a synergistic effect, despite  
467 MAML1 not having an individual impact. Very little is known about the interactions between  $\alpha$ -HPVs and  
468 MAML1, but our hypothesis of two distinct pools of HR E6 could potentially explain the effects described  
469 here. E6 promotes cell proliferation in a variety of ways, but its effects are limited in the absence of E6AP.  
470 Transfecting cells with both E6 and E6AP allows the viral oncoprotein to exert its typical functions, while  
471 transfection with MAML1 does not have the same effect, even though it does increase the overall stability  
472 of E6.

473         Despite the fact that we saw no significant effects of the interaction of MAML1 and E6 on cell  
474 proliferation in the overexpression experiments, it is well known that Notch signaling is involved in  
475 proliferation as well as cellular migration, and it could therefore very well be possible for E6 and MAML1  
476 to influence cell behavior in this manner. For this reason, we silenced either MAML1 or E6AP (or both) in  
477 HeLa cells with designated siRNAs, and also included siRNA against luciferase as a control. Forty-eight hrs  
478 after silencing the confluent cell monolayer was scratched with a pipette tip and photographed (Figure 10,  
479 left panel). Eighteen hrs later, the cells were photographed again, and the surface area of the wound was  
480 determined with the MRI wound-healing tool macro for the ImageJ software. By creating a gap in the cell  
481 monolayer, we were able to observe changes in the migratory/proliferation potential of cells at the edge  
482 of the gap depending on the silencing. Silencing E6AP led to a decrease in wound closure from 73% to 57%,  
483 most likely due to the consequential diminished amount of E6 driving proliferation and deregulating cell  
484 polarity (Figure 10, right panel). Surprisingly, considering that overexpressing MAML1 alone did not impact  
485 proliferation, silencing MAML1 decreased HeLa migratory/proliferation capacity to a similar degree as

486 silencing E6AP – i.e. from 73% to 64% (Figure 10, right panel). This could be due to the decline in the total  
487 amounts of E6 protein. Alternatively, this could also be an effect resulting from the loss of Notch signaling.  
488 It was a quite curious observation that, in contrast to what had been observed in our proliferation  
489 experiments, in this experimental setup E6AP and MAML1 did not act synergistically since the rate of  
490 migration/proliferation remained the same as with individually silenced E6AP and MAML1, i.e. migratory  
491 activity decreased from the 73% in controls to 64% in both treated samples (Figure 10, right panel).

## 492 Discussion

493  $\alpha$ -HPVs have been in the focus of HPV research for many years, mostly due to their impact on  
494 human health and the disease development, while  $\beta$ -HPVs have, thus far, been considered auxiliary factors  
495 in skin carcinogenesis, with the exception of HPV-38 [15]. Species from both  $\alpha$  and  $\beta$  genera use E6 and E7  
496 oncoproteins to remodel the cellular environment to suit viral needs, but in distinct and genus-specific  
497 ways. A recent manuscript emphasized these differences by demonstrating a clear preference of  $\alpha$ -E6  
498 oncoproteins to bind to E6AP, while E6 oncoproteins from the remaining four genera complex with MAML1  
499 [19]. Indeed, it is well-described that  $\beta$ -HPV E6s' binding to MAML1 has an inhibitory effect on Notch  
500 signaling and, subsequently, on keratinocyte differentiation. This effect is extremely important for the  
501 maintenance of a productive viral life cycle, considering that Notch signaling in keratinocytes regulates cell  
502 cycle progression [22,25]. Interestingly,  $\alpha$ -HPV-16 E6 was also found to bind to MAML1, but to a much  
503 lesser degree [19]. As the effect of Notch signaling in  $\alpha$ -HPV infections and carcinogenesis is poorly  
504 described, and furthermore, considering that MAML1 interaction was thought to be exclusive for  $\beta$ -HPVs,  
505 the biochemical basis of this potential interplay has not been explored in much detail up to present.

506 Our experiments now confirm the previously reported interaction between MAML1 and HPV-16  
507 E6, which is evidently weaker than the interaction between HPV-8 E6 and MAML1. This observation  
508 encouraged us to further investigate if other  $\alpha$ -E6s could also associate with MAML1. Using GST pull-down

509 assays, we demonstrated that, in addition to HPV-16 and HPV-8 E6s, -18 E6 and -11 E6 also interact with  
510 MAML1. We chose to examine these species because HPV-16 and HPV-18 are the most prominent HR HPVs,  
511 and HPV-11 is a common representative of LR mucosal type [1]. As expected, HPV-8 E6 was found to be  
512 the strongest interactor of MAML1, followed by HPV-18 E6 and -16 E6, and finally HPV-11 E6 which had  
513 the weakest overall indicating that both HR and LR mucosal HPVs bind to MAML1. Because of this very  
514 weak interaction between HPV-11 E6 and MAML1, we chose not to pursue this avenue further.

515         The main interaction partners of E6 serve to adapt the cellular milieu to viral replication,  
516 irrespective of the genera the E6 oncoproteins belong to. HR E6s hijack E6AP and form a stable complex  
517 with it, resulting in E6 protein stabilization. The stable complex is then directed by E6 towards a number of  
518 cellular targets important for the maintenance of a virus-optimized environment, ensuring a regulated  
519 turnover at the proteasome [41].  $\beta$ -PVs interact with MAML1 in order to block cell differentiation and cell-  
520 cycle arrest of target cells as completion of the viral life cycle is highly dependent on the host cell  
521 differentiation status [22,25]. Interestingly, both  $\alpha$ - and  $\beta$ -HPV E6 proteins utilize the same LXXLL motif to  
522 bind to E6AP and MAML1, respectively, and, as the impact of E6AP on E6 protein turnover is well defined,  
523 we sought to determine if MAML1 would induce a similar effect. By co-expressing MAML1, or E6AP as a  
524 control, together with the E6 oncoproteins of different  $\alpha$ - and  $\beta$ -HPVs, we demonstrated that MAML1 had  
525 an upregulatory effect on E6 protein expression levels, irrespective of the HPV genus. E6AP demonstrated  
526 positive effects on the stability on all  $\alpha$ -PVs examined, but had no effect on the protein stability of the  
527 analyzed  $\beta$ -PV E6, with the exception of HPV-24 E6 and HPV-38 E6. Previous reports have noted that these  
528 types interact with both MAML1 and E6AP, making it likely that, like  $\alpha$ -HPVs, they might also possess two  
529 pools of E6 proteins. [20]. The initial analyses were repeated in an E6AP-null background and these  
530 experiments yielded similar results. This allowed for the conclusion that the effects of MAML1 in inducing  
531 E6 oncoprotein stability were indeed mostly E6AP-independent. The stabilization effect of MAML1 on  $\beta$ -E6  
532 oncoproteins makes perfect sense, considering MAML1 utilization for Notch inhibition by  $\beta$ -HPV E6s, as

533 well as the absence of stabilization by E6AP, but the reasons behind  $\alpha$ -HPV E6 stabilization appear to be  
534 much more complex. One possible reason could be that  $\alpha$ -HPVs, like  $\beta$ -HPVs, use MAML1 to block the  
535 formation of the Notch ternary complex and thus consequently block the activation of Notch and  
536 keratinocyte differentiation. HR E6 oncoproteins could have evolved to use the same conserved interacting  
537 motif to maintain both their primary strong interaction with E6AP and the weaker secondary interaction  
538 with MAML1 in order to maximize their overall protein stability and the potential for viral propagation. It is  
539 also likely that each of these two interacting complexes might be required for establishing an optimal  
540 cellular environment for the virus to successfully complete its life cycle.

541         The LXXLL motif is exceedingly important for the binding of E6 to many cellular targets, including  
542 E6AP and MAML1, and disrupting the binding of E6 to this peptide leads to the inhibition of E6 downstream  
543 effects [45]. With some E6 oncoproteins, auxiliary interactions in the carboxyl-terminal HECT domain or a  
544 region in the amino terminus are required for E6-E6AP binding, and we do not know whether similar  
545 accessory regions are required for E6-MAML1 interactions [46]. That being said, not all E6 mutations  
546 completely inhibit the binding of E6 to its targets, and there is a certain degree of flexibility in respect to  
547 amino acid residues included, as far as E6 interaction capabilities with its targets are concerned. For this  
548 reason, we wanted to further examine whether E6 stabilization by MAML1 might be exclusively dependent  
549 on the LXXLL motif or if it might also require binding to additional regions of MAML1, and to determine  
550 how susceptible these interactions might be to mutations in the LXXLL motif [45,46]. Previous research has  
551 shown that mutating the aspartate residues of the MAML1 LXXLL motif to histidine decreases the binding  
552 of HPV-8 E6 to MAML1 and, consequently, the rate of Notch inhibition [32]. We assessed whether mutating  
553 the same residues (LDDLL to LHHLL) would lead to a decreased stability of HPV-8, -16 and -18 E6 proteins,  
554 or have an impact on binding to MAML1. Interestingly, HPV-8 and -18 E6s were still stabilized by the  
555 mutated MAML1, albeit to a lesser degree, while HPV-16 E6 was not. The MAML1 LHHLL was found to  
556 retain a weaker affinity for HPV-8 E6 and HPV-18 E6, indicating that binding to the motif is indeed required

557 for the interaction with E6, but it opens a possibility that broader peptide domains or specific neighboring  
558 amino acids may be involved in achieving the complete interaction. These results are in accordance with  
559 those of the GST pull-down assay, where in the comparison with HPV-18 E6, HPV-16 E6 demonstrated a  
560 weaker interaction with MAML1. It is therefore possible that their binding is somewhat different, as it is  
561 the case with E6AP [42], and that mutating the two aforementioned amino acid residues might be sufficient  
562 to completely disable the binding capacity of HPV-16 E6 to MAML1. Most surprisingly, HPV-16 E6 and HPV-  
563 18 E6 have shown opposing results, even though their biochemical behavior has thus far been considered  
564 identical. This again demonstrates that the interactions of different E6 oncoproteins, even of those of the  
565 same genus, cannot not be generalized and could have potentially different impacts on HPV-mediated  
566 pathogenesis.

567         Ectopic expression assays demonstrated that E6 binds to MAML1, and that this binding results in  
568 E6 protein stabilization. However, since overexpression experiments do not always translate entirely into  
569 naturally occurring systems, we aimed at determining whether the same effect can be observed in the cell  
570 lines that express E6 endogenously. Silencing MAML1 in an HPV-8 E6 expressing HT1080 fibrosarcoma cell  
571 line [17] decreased the amount of detectable 8 E6, while silencing E6AP had no effect. These results were  
572 expected, as it was previously described that E6AP does not interact with or impact a vast majority of  $\beta$ -  
573 HPV E6s [20]. Silencing endogenous MAML1 expression in HPV-18 positive HeLa cells resulted in the  
574 downregulation of E6 protein levels. Interestingly, this did not have any effect on some of the main E6  
575 functions, such as regulation of p53 protein turnover. E6 was stabilized at the protein level, as blocking the  
576 proteasomal turnover nullified the effect. We also confirmed that this effect was not HPV-18 E6 specific,  
577 since it was also seen in HPV-16 E6-positive CaSki cells. These results led us to believe that there are two  
578 distinct cellular pools of HR E6. One of these E6 pools binds to MAML1, resulting in E6 stabilization, but this  
579 complex appears not to be involved in some of the known E6/E6AP dependent functions. The remaining  
580 cellular E6 is E6AP-bound and plays a role in some of the previously characterized E6 oncogenic functions,

581 as demonstrated by our immunofluorescence experiments and the observed restoration of p53 levels  
582 following E6AP silencing. Likewise, we observed a downregulation of endogenous p53 protein level in the  
583 presence of ectopically expressed HPV-16 E6 alone or with E6AP, while overexpressing MAML1 with HPV-  
584 16 E6 led to restoration of initial p53 levels. This observation strongly indicates that overabundantly present  
585 MAML1 may occupy all available E6 molecules within the cell and prevent E6 from interacting with E6AP,  
586 and as such marking of p53 for proteasomal degradation. Furthermore, we wanted to expand our analysis  
587 by examining another well-defined E6 target, such as PDZ domain-containing protein DLG1. Unlike p53,  
588 which was previously found to be degraded exclusively in the presence of E6AP, an additional, currently  
589 unknown, E6AP-independent mechanism is involved in E6-mediated DLG1 degradation [34]. As expected,  
590 DLG1 was degraded in the presence of 16 E6, alone or in combination with E6AP, while no additional change  
591 in DLG1 level was detected when 16 E6 was overexpressed with MAML1, indicating that the E6 pool  
592 stabilized by MAML1 is not involved in regulation of DLG1 turnover.

593         Having established that silencing MAML1 affects E6 protein levels irrespective of the HPV genus,  
594 and that this regulation is proteasome-dependent, we wanted to further verify these results by determining  
595 the half-life of E6 in the presence or absence of MAML1. Ablating MAML1 caused a notable decrease in the  
596 half-life of both HPV-8 and -18 E6s, while silencing E6AP only decreased HPV-18 E6 half-life, confirming that  
597 there is only one cellular pool of HPV-8 E6, exclusively regulated by binding to MAML1. With HPV-18 E6,  
598 the synergistic impact of MAML1 and E6AP was also visible when both were silenced, as this silencing led  
599 to a further decrease in protein half-life, when compared with cells with individually silenced genes. These  
600 findings corroborate our two-pools hypothesis; when either MAML1 or E6AP are depleted HPV-18 E6 half-  
601 life is noticeably shorter than when both are present (Figure 11).

602         The binding of proteins to their interacting partners can lead to the blocking of their active or  
603 binding sites, or can induce shuttling of the entire complex to a new subcellular location, leading to  
604 modulations in protein functions. Consequently, we went on to determine whether E6 localization and the

605 area of accumulation might be changed by interacting with MAML1 in comparison with E6AP. HPV-16 and  
606 -18 E6 have previously been shown to be localized mostly in the nucleus and the ribosomal areas of the  
607 cytoplasm [36,47]. This localization may just be a snapshot of a more dynamic state of E6 protein  
608 localization within a cell, as there are reports indicating that the formation of a tertiary complex of HPV-18  
609 E6, p53 and E6AP causes protein shuttling from the nucleus to the cytoplasm and that the majority of p53  
610 is degraded in the cytoplasm [48]. MAML1 and E6AP are both usually found in the nucleus, but can be  
611 found in the cytoplasm as well. Interestingly, stabilizing HPV-16 E6 by MAML1 leads to a drastic increase of  
612 16 E6 localized in the nucleus and membranes, while stabilizing it by E6AP increases the E6 cytosolic  
613 fraction, indicating that the two different pools localize in different cellular compartments [20,42]. It is clear  
614 that MAML1 and E6AP do not stabilize HPV-16 E6 in the same manner. The increase of HPV-16 E6 in the  
615 nuclear fraction may impact E6 functions, as previously shown for HPV-18 E6, by exposing it to different  
616 binding partners [48]. On the other hand, considering the subcellular location of MAML1 and the lack of  
617 evidence for active protein shuttling, the likely explanation could be that MAML1 might simply increase the  
618 amount of protein present in the nuclear fraction because it stabilizes this particular pool and thus increases  
619 its total amount and activity in the nucleus. On the other hand, E6AP is used as a molecular tool by E6 for  
620 performing distinct cellular functions, mostly protein degradation in the cytoplasm, so the E6/E6AP  
621 complex is primarily found in that part of the cell.

622 Like HPV-16 E6, HPV-8 E6 has been previously found to be localized predominately in the nucleus  
623 and to a lesser extent, in the cytoplasm [47]. When examining HPV-8 E6 overexpressed in HEK-293 cells,  
624 we noticed again that the distribution of HPV-8 E6 changes depending on the presence of MAML1. When  
625 expressed alone, HPV-8 E6 is mostly found in the nucleus, as when expressed with E6AP which, in this case,  
626 served as a negative control for HPV-8 E6 distribution and confirmed that E6AP does not influence 8 E6  
627 cellular shuttling. When co-expressed with MAML1, we found HPV-8 E6 to be distributed in the cytosolic  
628 and nuclear fractions. This nuclear localization of HPV-8 E6 is most evident in immunofluorescence, where

629 cytoplasmic localization is less noticeable and silencing MAML1 leads to a much dimmer HPV-8 E6 signal,  
630 pointing towards the importance of MAML1 in HPV-8 E6 turnover. Considering that HPV-8 E6 interacts  
631 mostly with proteins located in the nucleus and cytoplasm, it would be of interest to see whether this  
632 binding has an effect on the binding of HPV-8 E6 to its other partners, and whether the presence or absence  
633 of MAML1 impacts the profile of the interacting partners of HPV-8 E6.

634 MAML1 binding clearly has a profound effect on E6 oncoprotein stability and localization of both  
635  $\alpha$ - and  $\beta$ -HPVs, but whether and how this interaction translates into biological functions is of great interest.  
636 Considering that the interaction of HPV-8 E6 with MAML1 has well-established biological consequences on  
637 Notch signaling, cell proliferation and keratinocyte differentiation, the focuses of this research were to  
638 elucidate biochemical and cellular effects of HR  $\alpha$ -HPVs complexing with MAML1 [25]. We overexpressed  
639 HPV-16 E6 and -18 E6 alone or in combination with MAML1, E6AP or both, in E6AP KO cells, in order to  
640 ensure that E6 stabilization would not be promoted by endogenous E6AP. We found that, when  
641 overexpressed in a cellular system, E6AP-mediated E6 stabilization leads to a statistically significant  
642 increase of cell proliferation, as we and others have previously described [39]. MAML1-mediated  
643 stabilization of E6 had no discernible effects on cell proliferation, when compared with the effects of HR  
644 HPV E6 proteins alone. Remarkably, when HPV-16 E6 or -18 E6 were co-expressed with both MAML1 and  
645 E6AP, the effect on cell proliferation was much stronger than that of E6AP alone. This effect could be due  
646 to MAML1-mediated increase in E6 stability which might, in turn, increase the amount of E6 molecules  
647 present within a given cell and, as a long-term consequence, increase the amount of E6 available for  
648 interaction with E6AP. When this concept is transferred to a naturally occurring cell line, such as Hela,  
649 silencing E6AP by RNA interference leads to decreased wound healing, probably due to growth suppression  
650 by p53, whose protein level within the cell increases as a consequence of decreased E6 presence [49]. In  
651 the same system, inhibition of MAML1 leads to a decrease in wound healing, comparable to that of  
652 abrogated E6AP. Interestingly, the same effect has previously been reported and associated with inhibition

653 of Notch signaling in HeLa cells, but the authors offered no further explanation as to how this came to be  
654 [50]. It is possible that maintaining E6 stability with MAML1 is indispensable for sustaining HeLa cell viability,  
655 but it is likely that completely abrogating Notch signaling by silencing MAML1 leads to a growth arrest, as  
656 Notch signaling is very finely tuned and both under- and over-modulation can be detrimental for cell  
657 proliferation [50,51]. Interestingly, in the same experimental setting, MAML1 and E6AP do not exhibit  
658 synergistic effects, as silencing both does not lead to an additional decrease in the percentage of the wound  
659 healed. MAML1 could therefore contribute to an increase in absolute amounts of E6 within the cell. In this  
660 context, MAML1 silencing would influence proliferation only through decreasing the availability of E6 for  
661 binding to E6AP, through which it exerts most of its functions. HeLa proliferation is only partially dependent  
662 on the effects of E6, which also means that reducing the amount of E6 by any means will only influence the  
663 cellular phenotype to a limited degree. Considering that E7 is considered to be the main driver of  
664 proliferation combined with the fact that it is still abundantly present in HeLa cells could be the explanation  
665 for the observed effects [52].

666 Our research focused on the previously uninvestigated effects that E6s interacting partners have  
667 on its stability and function. Here, we show that a well-defined interaction of  $\beta$ -HPVs with MAML1 serves  
668 to increase E6 protein stability, in addition to inhibiting Notch signaling and abrogating keratinocyte  
669 differentiation. Moreover, we show for the first time that a formerly overlooked, LXXLL motif-dependent  
670 interaction of HR  $\alpha$ -HPVs with MAML1 has a stabilizing effect on E6s. The increased stability of E6 does not  
671 translate to an increase in E6-mediated degradation efficiencies for some of its most common targets.  
672 However, importantly, it seemingly has an impact on cell migration and proliferation, presumably via a still  
673 undiscovered mechanism. Taken together, and as summarized in Figure 11, our results imply the existence  
674 of two distinct pools of HR E6 oncoproteins; E6/E6AP being well-characterized, and E6/MAML1, whose  
675 functions are currently being investigated further.

676 **Author Contributions**

677 Conceived and designed the experiments: JS, AĐ, BA, VT; Performed the experiments: JS, AĐ, MH,  
678 VF; Analyzed the data: JS, AĐ, VF, BA, VT; Contributed reagents/materials/analysis tools: MH, BA, MT, LB;  
679 Wrote the paper: JS, AĐ, VT. All authors read and approved the final version of the manuscript.

680

681           **Acknowledgements**

682           We are very grateful to Karl Münger for kindly providing pCMV2-FLAG-MAML1 and pCMV2-FLAG-  
683 MAML1 LHHLL expression plasmids, and to Allan Albig for kindly providing pCS2 MYC-MAML1 expression  
684 plasmid. We also thank to Sandra Sobočanec for all technical support concerning western blot analyses.  
685 This work was supported by the Croatian Science Foundation (grant no. 2246) and by an ICGEB Early Career  
686 Return Grant (grant no. CRP/16/018) to VT. BA and MH were supported by the German Research  
687 Foundation (AK 42/11-1). BA and VT gratefully acknowledge travel support from the German Academic  
688 Exchange Service (Grant no. 57447417) and the Croatian Ministry of Science and Education.

689           **Conflicts of interest**

690           Authors declare no conflict of interest.

691           **Data availability statement**

692           All relevant data are within the manuscript and its Supporting Information files.

693

694  
695  
696  
697  
698  
699  
700  
701  
702  
703  
704  
705  
706  
707  
708  
709  
710  
711  
712  
713  
714  
715

## References

1. World Health Organisation. INTERNATIONAL AGENCY FOR RESEARCH ON CANCER IARC Monographs on the Evaluation of Carcinogenic Risks to Humans VOLUME 90 Human Papillomaviruses. IARC Monographs On The Evaluation Of Carcinogenic Risks To Humans. 2007. Available: <http://scholar.google.com/scholar?hl=en&btnG=Search&q=intitle:Monographs+on+the+Evaluation+of+Carcinogenic+Risks+to+Humans+VOLUME+90+Human+Papillomaviruses#0>
2. Zur Hausen H. Papillomaviruses and cancer: From basic studies to clinical application. *Nature Reviews Cancer*. 2002. pp. 342–350. doi:10.1038/nrc798
3. Bouvard V, Baan R, Straif K, Grosse Y, Secretan B, El Ghissassi F, et al. A review of human carcinogens—Part B: biological agents. *The Lancet Oncology*. 2009. pp. 321–322. doi:10.1016/S1473-2045(09)70096-8
4. Li N, Franceschi S, Howell-Jones R, Snijders PJF, Clifford GM. Human papillomavirus type distribution in 30,848 invasive cervical cancers worldwide: Variation by geographical region, histological type and year of publication. *Int J Cancer*. 2011;128: 927–935. doi:10.1002/ijc.25396
5. Dyson N, Howley P, Munger K, Harlow E. The human papilloma virus-16 E7 oncoprotein is able to bind to the retinoblastoma gene product. *Science* (80- ). 1989;243: 934–937. doi:10.1126/science.2537532
6. Scheffner M, Werness BA, Huibregtse JM, Levine AJ, Howley PM. The E6 oncoprotein encoded by human papillomavirus types 16 and 18 promotes the degradation of p53. *Cell*. 1990;63: 1129–1136. doi:10.1016/0092-8674(90)90409-8
7. Morris EJ, Dyson NJ. Retinoblastoma protein partners. *Advances in Cancer Research*. Academic Press Inc.; 2001. pp. 1–54. doi:10.1016/S0065-230X(01)82001-7

- 716 8. Münger K, Werness BA, Dyson N, Phelps WC, Harlow E, Howley PM. Complex formation of human  
717 papillomavirus E7 proteins with the retinoblastoma tumor suppressor gene product. *EMBO J.* 8,  
718 4099–105. E7 proteins. *EMBO J.* 1989;8: 4099–105. Available:  
719 <http://www.pubmedcentral.nih.gov/articlerender.fcgi?artid=401588&tool=pmcentrez&rendertype=abstract>  
720 e=abstract
- 721 9. Scheffner M, Huibregtse JM, Vierstra RD, Howley PM. The HPV-16 E6 and E6-AP complex functions  
722 as a ubiquitin-protein ligase in the ubiquitination of p53. *Cell.* 1993;75: 495–505. doi:10.1016/0092-  
723 8674(93)90384-3
- 724 10. Martinez-Zapien D, Ruiz FX, Poirson J, Mitschler A, Ramirez J, Forster A, et al. Structure of the  
725 E6/E6AP/p53 complex required for HPV-mediated degradation of p53. *Nature.* 2016;529: 541–545.  
726 doi:10.1038/nature16481
- 727 11. Tomaić V, Pim D, Banks L. The stability of the human papillomavirus E6 oncoprotein is E6AP  
728 dependent. *Virology.* 2009;393: 7–10. doi:10.1016/j.virol.2009.07.029
- 729 12. Thomas M, Narayan N, Pim D, Tomaić V, Massimi P, Nagasaka K, et al. Human papillomaviruses,  
730 cervical cancer and cell polarity. *Oncogene.* 2008;27: 7018–7030. doi:10.1038/onc.2008.351
- 731 13. Pim D, Bergant M, Boon SS, Ganti K, Kranjec C, Massimi P, et al. Human papillomaviruses and the  
732 specificity of PDZ domain targeting. *FEBS J.* 2012;279: 3530–3537. doi:10.1111/j.1742-  
733 4658.2012.08709.x
- 734 14. Quint KD, Genders RE, De Koning MNC, Borgogna C, Gariglio M, Bavinck JNB, et al. Human Beta-  
735 papillomavirus infection and keratinocyte carcinomas. *J Pathol.* 2015;235: 342–354.  
736 doi:10.1002/path.4425
- 737 15. Tommasino M. The biology of beta human papillomaviruses. *Virus Research.* Elsevier B.V.; 2017. pp.

- 738 128–138. doi:10.1016/j.virusres.2016.11.013
- 739 16. Jackson S, Storey A. E6 proteins from diverse cutaneous HPV types inhibit apoptosis in response to  
740 UV damage. *Oncogene*. 2000;19: 592–598. doi:10.1038/sj.onc.1203339
- 741 17. Hufbauer M, Cooke J, van der Horst GTJ, Pfister H, Storey A, Akgül B. Human papillomavirus  
742 mediated inhibition of DNA damage sensing and repair drives skin carcinogenesis. *Mol Cancer*.  
743 2015;14: 183. doi:10.1186/s12943-015-0453-7
- 744 18. Caldeira S, Zehbe I, Accardi R, Malanchi I, Dong W, Giarre M, et al. The E6 and E7 Proteins of the  
745 Cutaneous Human Papillomavirus Type 38 Display Transforming Properties. *J Virol*. 2003;77: 2195–  
746 2206. doi:10.1128/jvi.77.3.2195-2206.2003
- 747 19. Brimer N, Drews CM, Vande Pol SB. Association of papillomavirus E6 proteins with either MAML1 or  
748 E6AP clusters E6 proteins by structure, function, and evolutionary relatedness. *PLoS Pathog*.  
749 2017;13: 1–27. doi:10.1371/journal.ppat.1006781
- 750 20. Thomas M, Tomaić V, Pim D, Myers MP, Tommasino M, Banks L. Interactions between E6AP and E6  
751 proteins from alpha and beta HPV types. *Virology*. 2013;435: 357–362.  
752 doi:10.1016/j.virol.2012.11.004
- 753 21. Rodrigues C, Joy LR, Sachithanandan SP, Krishna S. Notch signalling in cervical cancer. *Exp Cell Res*.  
754 2019;385: 111682. doi:10.1016/j.yexcr.2019.111682
- 755 22. Lowell S, Jones P, Le Roux I, Dunne J, Watt FM. Stimulation of human epidermal differentiation by  
756 delta-notch signalling at the boundaries of stem-cell clusters. *Curr Biol*. 2000;10: 491–500.  
757 doi:10.1016/s0960-9822(00)00451-6
- 758 23. Kelley ML, Keiger KE, Lee CJ, Huibregtse JM. The Global Transcriptional Effects of the Human  
759 Papillomavirus E6 Protein in Cervical Carcinoma Cell Lines Are Mediated by the E6AP Ubiquitin

- 760 Ligase. *J Virol.* 2005;79: 3737–3747. doi:10.1128/jvi.79.6.3737-3747.2005
- 761 24. Thatte J, Banks L. Human Papillomavirus 16 (HPV-16), HPV-18, and HPV-31 E6 Override the Normal  
762 Phosphoregulation of E6AP Enzymatic Activity. *J Virol.* 2017;91. doi:10.1128/jvi.01390-17
- 763 25. Brimer N, Lyons C, Wallberg AE, Vande Pol SB. Cutaneous papillomavirus E6 oncoproteins associate  
764 with MAML1 to repress transactivation and NOTCH signaling. *Oncogene.* 2012;31: 4639–4646.  
765 doi:10.1038/onc.2011.589
- 766 26. Tan MJA, White EA, Sowa ME, Harper JW, Aster JC, Howley PM. Cutaneous  $\beta$ -human papillomavirus  
767 E6 proteins bind Mastermind-like coactivators and repress Notch signaling. *Proc Natl Acad Sci U S*  
768 *A.* 2012;109: 1473–1480. doi:10.1073/pnas.1205991109
- 769 27. Meyers JM, Spangle JM, Munger K. The Human Papillomavirus Type 8 E6 Protein Interferes with  
770 NOTCH Activation during Keratinocyte Differentiation. *J Virol.* 2013;87: 4762–4767.  
771 doi:10.1128/jvi.02527-12
- 772 28. Matlashewski G, Schneider J, Banks L, Jones N, Murray A, Crawford L. Human papillomavirus type  
773 16 DNA cooperates with activated ras in transforming primary cells. *EMBO J.* 1987;6: 1741–1746.
- 774 29. Pim D, Massimi P, Banks L. Alternatively spliced HPV-18 E6\* protein inhibits E6 mediated  
775 degradation of p53 and suppresses transformed cell growth. *Oncogene.* 1997;15: 257–264.  
776 doi:10.1038/sj.onc.1201202
- 777 30. Tomaic V, Pim D, Thomas M, Massimi P, Myers MP, Banks L. Regulation of the Human Papillomavirus  
778 Type 18 E6/E6AP Ubiquitin Ligase Complex by the HECT Domain-Containing Protein EDD. *J Virol.*  
779 2011;85: 3120–3127. doi:10.1128/jvi.02004-10
- 780 31. Thomas M, Massimi P, Navarro C, Borg J-PP, Banks L. The hScrib/Dlg apico-basal control complex is  
781 differentially targeted by HPV-16 and HPV-18 E6 proteins. *Oncogene.* 2005;24: 6222–6230.

- 782 doi:10.1038/sj.onc.1208757
- 783 32. Meyers JM, Uberoi A, Grace M, Lambert PF, Munger K. Cutaneous HPV8 and MmuPV1 E6 Proteins  
784 Target the NOTCH and TGF- $\beta$  Tumor Suppressors to Inhibit Differentiation and Sustain Keratinocyte  
785 Proliferation. *PLoS Pathog.* 2017;13: 1–29. doi:10.1371/journal.ppat.1006171
- 786 33. LaFoya B, Munroe JA, Pu X, Albig AR. Src kinase phosphorylates Notch1 to inhibit MAML binding. *Sci*  
787 *Rep.* 2018;8: 15515. doi:10.1038/s41598-018-33920-y
- 788 34. Vats A, Thatte J, Banks L. Identification of E6AP-independent degradation targets of HPV E6. *J Gen*  
789 *Virol.* 2019;100: 1674–1679. doi:10.1099/jgv.0.001331
- 790 35. Taute S, Böhnke P, Sprissler J, Buchholz S, Hufbauer M, Akgül B, et al. The Protein Tyrosine  
791 Phosphatase H1 PTPH1 Supports Proliferation of Keratinocytes and is a Target of the Human  
792 Papillomavirus Type 8 E6 Oncogene. *Cells.* 2019;8. doi:10.3390/cells8030244
- 793 36. Ganti K, Massimi P, Manzo-merino J, Tomai V, Pim D, Banks L, et al. Interaction of the Human  
794 Papillomavirus E6 Oncoprotein with Sorting Nexin 27 Modulates Endocytic Cargo Transport  
795 Pathways. *PLoS Pathog.* 2016;12: e1005854–e1005854. doi:10.1371/journal.ppat.1005854
- 796 37. Schneider CA, Rasband WS, Eliceiri KW. NIH Image to ImageJ: 25 years of Image Analysis HHS Public  
797 Access. *Nat Methods.* 2012;9: 671–675. doi:10.1038/nmeth.2089
- 798 38. Szalmás A, Tomaić V, Basukala O, Massimi P, Mittal S, Kónya J, et al. The PTPN14 Tumor Suppressor  
799 Is a Degradation Target of Human Papillomavirus E7. *J Virol.* 2017;91. doi:10.1128/jvi.00057-17
- 800 39. Saidu NEB, Filić V, Thomas M, Sarabia-Vega V, Đukić A, Miljković F, et al. PDZ Domain-Containing  
801 Protein NHERF-2 Is a Novel Target of Human Papillomavirus 16 (HPV-16) and HPV-18. *J Virol.*  
802 2019;94. doi:10.1128/JVI.00663-19

- 803 40. Thomas M, Myers MP, Massimi P, Guarnaccia C, Banks L. Analysis of Multiple HPV E6 PDZ  
804 Interactions Defines Type-Specific PDZ Fingerprints That Predict Oncogenic Potential. *PLoS Pathog.*  
805 2016;12: 1–21. doi:10.1371/journal.ppat.1005766
- 806 41. Đukić A, Lulić L, Thomas M, Skelin J, Saidu NEB, Grce M, et al. HPV oncoproteins and the ubiquitin  
807 proteasome system: A signature of malignancy? *Pathogens.* MDPI AG; 2020.  
808 doi:10.3390/pathogens9020133
- 809 42. Huibregtse JM, Scheffner M, Howley PM. Cloning and expression of the cDNA for E6-AP, a protein  
810 that mediates the interaction of the human papillomavirus E6 oncoprotein with p53. *Mol Cell Biol.*  
811 1993;13: 775–784. doi:10.1128/mcb.13.2.775
- 812 43. Kao WH, Beaudenon SL, Talis AL, Huibregtse JM, Howley PM. Human Papillomavirus Type 16 E6  
813 Induces Self-Ubiquitination of the E6AP Ubiquitin-Protein Ligase. *J Virol.* 2000;74: 6408–6417.  
814 doi:10.1128/jvi.74.14.6408-6417.2000
- 815 44. Androphy EJ, Hubbert NL, Schiller JT, Lowy DR. Identification of the HPV-16 E6 protein from  
816 transformed mouse cells and human cervical carcinoma cell lines. *EMBO J.* 1987;6: 989–992.  
817 doi:10.1002/j.1460-2075.1987.tb04849.x
- 818 45. Zanier K, Charbonnier S, Ould A, Ould M, Alastair G, Ferrario MG, et al. Structural basis for hijacking  
819 of cellular LxxLL motifs by papillomavirus E6 oncoproteins. *Science (80- ).* 2013;339: 694–698.  
820 doi:10.1126/science.1229934.Structural
- 821 46. Drews CM, Brimer N, Vande Pol SB. Multiple regions of E6AP (UBE3A) contribute to interaction with  
822 papillomavirus E6 proteins and the activation of ubiquitin ligase activity. *PLoS Pathog.* 2020;16: 1–  
823 25. doi:10.1371/journal.ppat.1008295
- 824 47. Mesplede T, Gagnon D, Bergeron-Labrecque F, Azar I, Senechal H, Coutlee F, et al. p53 Degradation

- 825 Activity, Expression, and Subcellular Localization of E6 Proteins from 29 Human Papillomavirus  
826 Genotypes. *J Virol.* 2012;86: 94–107. doi:10.1128/jvi.00751-11
- 827 48. Stewart D, Ghosh A, Matlashewski G. Involvement of Nuclear Export in Human Papillomavirus Type  
828 18 E6-Mediated Ubiquitination and Degradation of p53. *J Virol.* 2005;79: 8773–8783.  
829 doi:10.1128/jvi.79.14.8773-8783.2005
- 830 49. Hengstermann A, D’silva MA, Kuballa P, Butz K, Hoppe-Seyley F, Scheffner M. Growth suppression  
831 induced by downregulation of E6-AP expression in human papillomavirus-positive cancer cell lines  
832 depends on p53. *J Virol.* 2005;79: 9296–9300. doi:10.1128/JVI.79.14.9296-9300.2005
- 833 50. Yu H, Zhao X, Huang S, Jian L, Qian G, Ge S. Blocking Notch1 signaling by RNA interference can induce  
834 growth inhibition in HeLa cells. *Int J Gynecol Cancer.* 2007;17: 511–516.  
835 doi:https://doi.org/10.1111/j.1525-1438.2007.00813.x
- 836 51. Talora C, Cialfi S, Segatto O, Morrone S, Kim Choi J, Frati L, et al. Constitutively active Notch1 induces  
837 growth arrest of HPV-positive cervical cancer cells via separate signaling pathways. *Exp Cell Res.*  
838 2005;305: 343–354. doi:https://doi.org/10.1016/j.yexcr.2005.01.015
- 839 52. Jones DL, Alani RM, Münger K. The human papillomavirus E7 oncoprotein can uncouple cellular  
840 differentiation and proliferation in human keratinocytes by abrogating p21Cip1-mediated inhibition  
841 of cdk2. *Genes Dev.* 1997;11: 2101–2111. doi:10.1101/gad.11.16.2101

842

843

844 **Figure legends**

845 **Fig. 1.  $\alpha$ - and  $\beta$ - HPV E6 oncoproteins bind to MAML1.** A) HEK-293 cells were transfected with HA-  
846 tagged HPV-16 E6 or HPV-8 E6 alone or in combination with FLAG-tagged MAML1. Transfected cells were  
847 harvested, resuspended in lysis buffer and incubated with anti-HA beads on a rotating wheel at RT. The  
848 beads were extensively washed and co-immunoprecipitated complexes were subjected to western blot  
849 analysis with anti-FLAG antibody and compared with the amount of MAML1 present in 10% of the input.  
850 Dotted line divides two different exposures of the same membrane. B) Extracts from C33A cells, transiently  
851 transfected with either empty vector or plasmids coding for FLAG-16E6 were incubated with anti-FLAG  
852 beads. Co-immunoprecipitated MAML1 and HPV-16 E6 and 10% of the input extracts were subjected to  
853 western blots with specific antibodies. Equal protein loading was confirmed by immunoblotting for GAPDH.  
854 \* immunoglobulin light chain. C) HEK-293 cells were transfected with FLAG-tagged MAML1. After 24hrs,  
855 the cells were harvested, and the cell lysates were incubated with 16 E6, 18 E6, 8 E6 and 11 E6 GST fusion  
856 proteins. GST alone was included as a control. After extensive washing, bound MAML1 was detected by  
857 western blotting using anti-FLAG antibody and compared to the amount of MAML1 present in 10% of the  
858 input. The lower gel shows the positions of purified GST proteins used in the pulldowns visualized by  
859 Ponceau staining.

860 **Fig. 2. MAML1 stabilizes E6 oncoproteins from both  $\alpha$ - and  $\beta$ - HPV types.** A) HEK-293 cells and B)  
861 HEK-293 E6AP KO cells were transfected with HA-tagged HPV-8, -12, -14, -16, -18, -24, -33 and -38 E6 alone  
862 or in combination with either FLAG- or Myc-tagged MAML1 or E6AP. After 24hrs cells were harvested and  
863 isolated proteins from complete cell lysates separated on SDS-page, detected by anti-FLAG, anti-Myc and  
864 anti-HA antibodies and visualized by chemiluminescence. B-galactosidase (LacZ) was used as the control to  
865 monitor transfection efficiency and loading. Densitometric analysis was performed with ImageJ software.  
866 The band densities were first normalized for background for each of the samples after which relative  
867 expression was calculated by dividing E6 normalized density with LacZ normalized density. Average relative

868 expressions of control E6s were calculated and all other relative E6 expressions were compared to it in  
869 order to obtain E6 fold change. LOG2 of that fold change is depicted on the bar chart so that the increase  
870 in intensity is seen as a positive value and the decrease as a negative value. Each experiment was repeated  
871 at least three times.

872 **Fig. 3. E6 protein stabilization is MAML1 LXXLL motif dependent.** A) HEK-293 and HEK-293 E6AP KO  
873 cells were transfected with HA-tagged HPV-8, -11, -16 and -18 E6 alone or in combination with FLAG-tagged  
874 MAML1 or FLAG-tagged MAML1 mutant (MAML1 LHHLL). After 24hrs cells were harvested and isolated  
875 proteins from complete cell lysates were separated on SDS-page and analyzed by western Blotting. E6,  
876 MAML1 and MAML1 LHHLL were detected by anti-HA and anti-FLAG antibodies. B-galactosidase (LacZ) was  
877 used as the control for the transfection efficiency and loading. B) HEK-293 cells were transfected with HA-  
878 tagged HPV-8 E6 alone or in combination with FLAG-tagged MAML1 or FLAG-tagged MAML1 mutant.  
879 Transfected cells were harvested, resuspended in lysis buffer and incubated with anti-HA beads on a  
880 rotating wheel at RT. The beads were extensively washed and co-immunoprecipitated complexes subjected  
881 to western blot analysis with anti-FLAG antibody and compared to the amount of MAML1 or MAML1 LHHLL  
882 present in 10% of the input.

883 **Fig. 4. HPV E6 protein stability in CaSki, HeLa and HPV-8 E6 expressing HT1080 cells is MAML1**  
884 **dependent.** A) HeLa cells, B) CaSki and C) HT1080 HPV-8 E6 cells were transfected with individual siRNA  
885 against Luciferase (siLuc), or a pool of siRNA against MAML1 (siMAML1) or siRNA against E6AP (siE6AP).  
886 Forty-eight hrs later, proteasome inhibitor Bortezomib (BTZ) was added as indicated and the cells were  
887 then incubated for a further 24hrs after which they were harvested, separated on SDS-page, and detected  
888 by western blotting with anti-MAML1, anti-E6AP, anti-HPV-18 E6 (B) and anti-FLAG antibodies (C) followed  
889 by HRP-coupled anti-mouse and anti-rabbit antibodies and ECL detection.  $\beta$ -actin was used as internal  
890 control to monitor protein loading.

891 **Fig. 5. MAML1 stabilizes a distinctive cellular pool of HPV-18 E6 and an exclusive single cellular pool**  
892 **of HPV-8 E6.** (A and B) HeLa cells and (C and D) HT1080 8 E6 cells were transfected with indicated siRNAs.  
893 Seventy-two hrs post transfection the cells were fixed and stained with antibodies against MAML1 and  
894 E6AP to determine the silencing efficiency; p53 as readout for 18 E6 ablation; and FLAG (HPV-8 E6). Anti-  
895 mouse and rabbit secondary antibodies conjugated to Alexa Fluor 488 or rhodamine red were used to  
896 detect the primary antibodies, and nuclei were visualized with DAPI. Scale bars 10  $\mu$ m; the white arrows  
897 point towards cells of interest.

898 **Fig. 6. E6/MAML1 complex does not induce p53 and DLG1 degradation.** HEK-293 E6AP KO cells  
899 were transfected with A) p53 or B) HA-tagged DLG1, in combination with HA-tagged 16 E6 alone or in  
900 combination with either FLAG-tagged MAML1 or E6AP. After 24hrs the cells were harvested and isolated  
901 proteins from complete cell lysates were separated on SDS-page, detected by HRP-linked anti-HA or anti-  
902 p53 antibodies with an appropriate secondary antibody, after which the proteins were visualized by  
903 chemiluminescence.  $\beta$ -galactosidase (LacZ) was used as control to monitor transfection efficiency and  
904 loading. Densitometric analysis was performed with ImageJ software. Band densities were first normalized  
905 for background for each of the samples, after which relative expression was calculated by dividing p53 or  
906 DLG1 normalized density with LacZ normalized density. p53 or DLG1 average normalized relative expression  
907 was calculated for control samples, and all normalized relative expressions were compared to it. Fold  
908 change was obtained by dividing the relative expression of p53 or DLG1 in co-transfected samples with  
909 average relative expression of samples transfected alone. Each experiment was repeated at least four  
910 times.

911 **Fig. 7. HPV E6 protein turnover is regulated by MAML1.** (A) HeLa cells and (B) HT1080 8 E6 cells  
912 were transfected with siRNA against Luciferase (siLuc), MAML1 (siMAML1) and E6AP (siE6AP) alone or in  
913 combination. Seventy-two hrs later the cells were treated with Cycloheximide prior to harvesting at the  
914 time points as indicated. E6 protein expression levels were analyzed by western blotting with anti-MAML1,

915 anti-E6AP, anti-18 E6 (A) and anti-FLAG antibodies (B) followed by HRP-coupled anti-mouse and anti-rabbit  
916 antibodies and ECL detection.  $\beta$ -actin was used as internal control to monitor protein loading.  
917 Densitometric analysis was performed with ImageJ software. Band intensities were first normalized for  
918 background for each of the samples after which relative expression was calculated by dividing E6  
919 normalized density with  $\beta$ -actin normalized density. The initial band intensity of E6 was taken as 100%, and  
920 the density at other time points were calculated as percentage of the starting amount. The experiment was  
921 repeated at least three times. The results obtained are depicted in the graph (lower panel).

922 **Fig. 8. MAML1 causes changes in 16 E6 and 8 E6 cellular accumulation.** HEK-293 cells were  
923 transfected with HA-tagged HPV-16 E6 or HPV-8 E6 alone or in combination with either FLAG-tagged or  
924 myc-tagged MAML1 or E6AP. After 24hrs, the protein lysates were separated into the cytosolic (C),  
925 membrane (M), nucleic (N) and microtubule (T) cellular fractions by ProteoExtract® Subcellular Proteome  
926 Extraction Kit. The fractionated proteins were separated on SDS-PAGE and E6 was detected by western  
927 blotting with HRP-linked anti-HA antibody, while MAML1 was detected with anti-FLAG or anti-myc  
928 antibodies. The protein fraction purity was determined by incubation with specific antibodies (MCM7 for  
929 cytoplasm, GAPDH for membrane, histone H3 for nucleus and vimentin for cytoskeleton).

930 **Fig. 9. MAML1 and E6AP cooperate in increasing E6-dependent cellular proliferation.** HEK-293  
931 E6AP KO cells were transfected with HA-tagged HPV-16 E6 or HPV-18 E6, alone or in combination with  
932 FLAG-tagged MAML1, E6AP or both. The cells were also transfected with pCDNA3, used as a negative  
933 control, and  $\beta$ -galactosidase (LacZ) as an internal standard to monitor transfection efficiency and loading.  
934 Twenty-four hrs after transfection, the cells were detached, counted and seeded in quadruplicates in a 96  
935 well plate ( $5 \times 10^4$  cells per well), after which they were grown for a further 48hrs. Uptibblue was then added  
936 to the wells and the absorbance at 570 nm and 595 nm was measured 5hrs later. The percentage of  
937 Uptibblue reduction was calculated following manufacturer's instructions and it responds to the rate of  
938 proliferation. The average of at least three experiments is depicted on the graph, along with standard

939 deviations. Significance was determined by student's t-test, with  $p < 0.05$  taken as significant, and marked  
940 with \* above the bar ( $p < 0.01$  marked with \*\*).

941 **Fig. 10. Silencing MAML1 impacts cell migration in HPV-18 positive cells.** HeLa cells were  
942 transfected with individual siRNAs either against Luciferase (siLuc), against MAML1 (siMAML1) or against  
943 E6AP (siE6AP). Forty-eight hrs later, a wound scratch was made in the cell monolayer, the cells were washed  
944 and photographed (left panel). Eighteen hrs after scratching, the cells were photographed again (left  
945 panel). The surface area of the wounds was calculated with the MRI wound healing tool macro for ImageJ  
946 software, and the significance in the surface area difference between treatments was determined by  
947 student's t-test, with  $p < 0.05$  taken as significant and marked with \* ( $p < 0.01$  marked with \*\*) (right panel).  
948 All experiments were repeated at least four times.

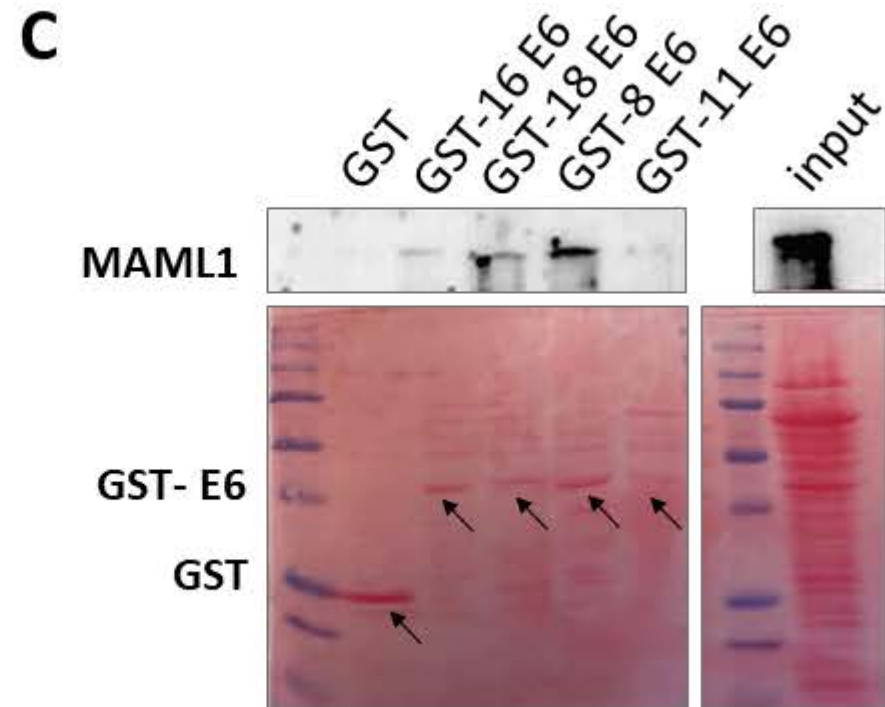
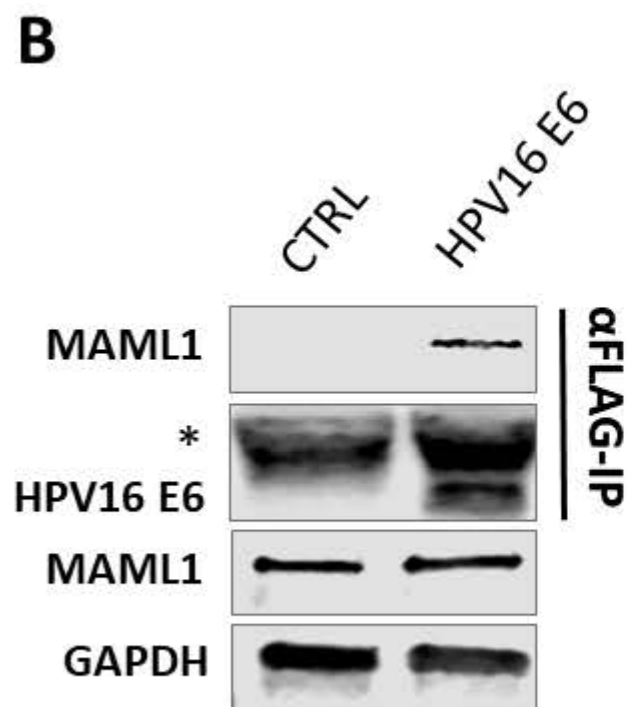
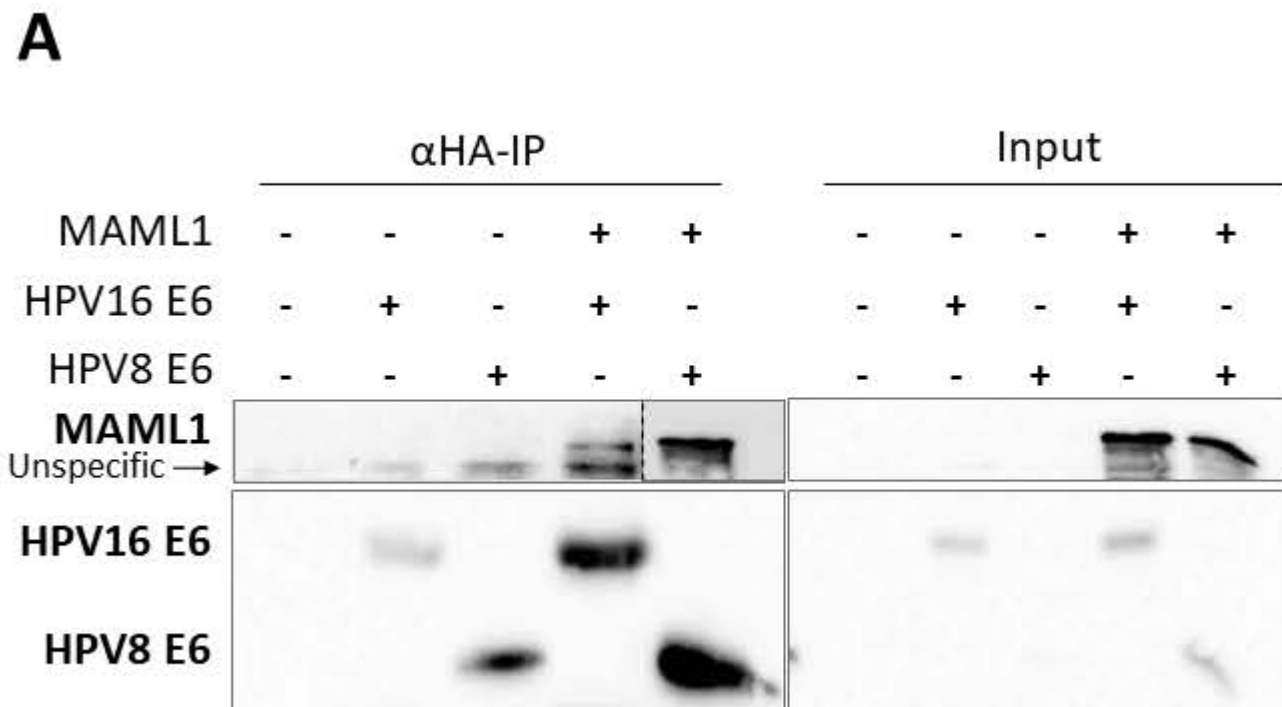
949 **Fig. 11. Working model for  $\alpha$ -HPV E6 and  $\beta$ -HPV E6 interplay with MAML1.** While majority of  $\beta$ -E6  
950 oncoproteins bind exclusively to MAML1 (right),  $\alpha$ -E6 oncoproteins bind either MAML1 or E6AP (left).  
951 MAML1 binding increases both mucosal and cutaneous E6 protein stability, impacts cell migration in HPV-  
952 18 positive background, but it does not influence HR mucosal E6 target degradation.

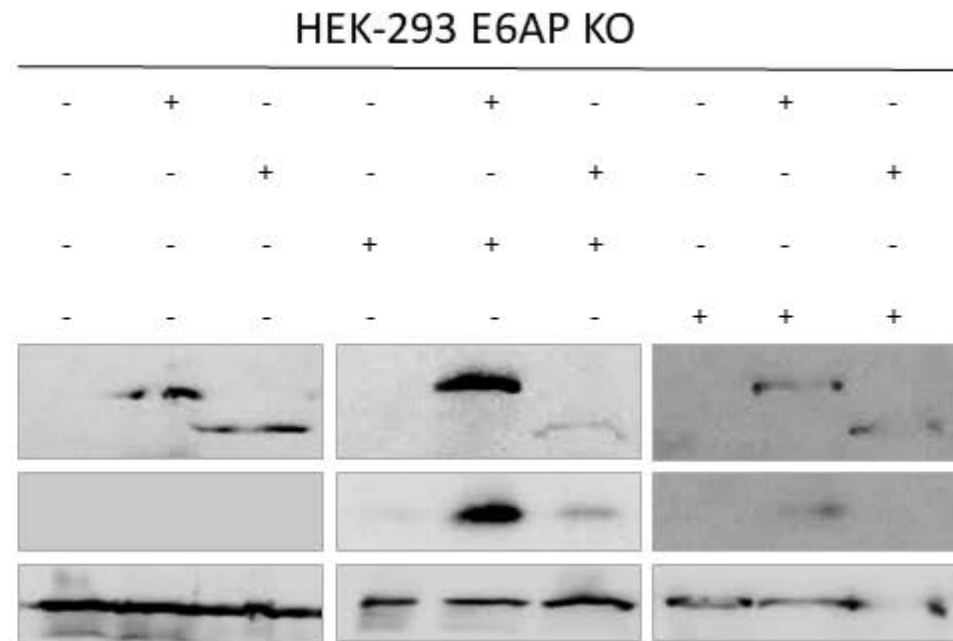
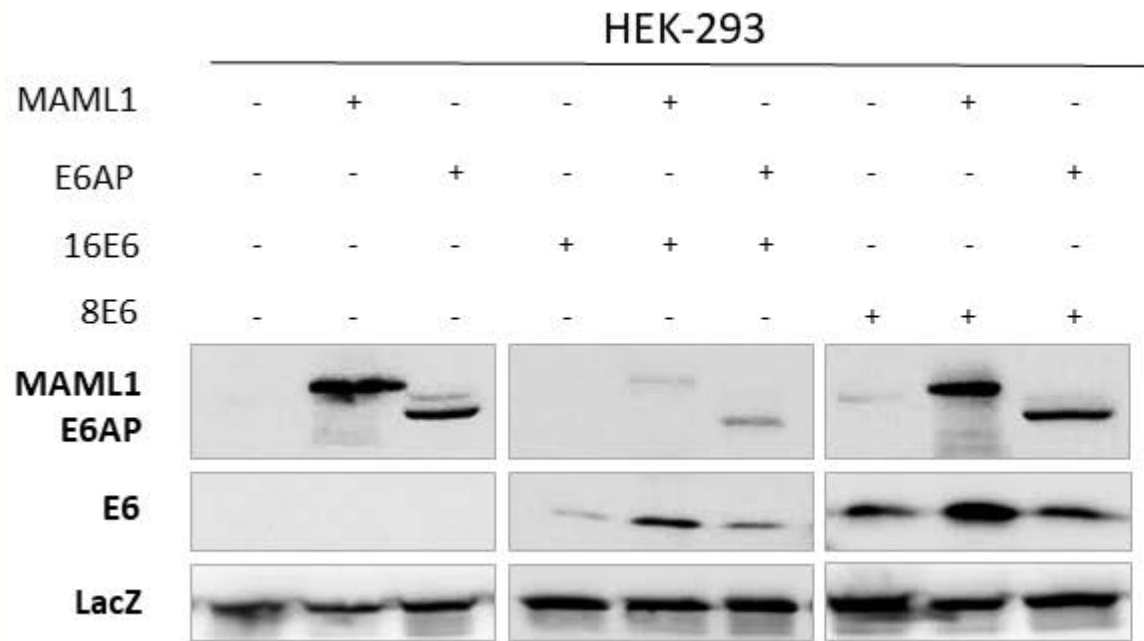
953 **Supp. Fig. 1. Negative controls for Figure 2.** HEK-293 cells (left panel) and HEK-293 E6AP KO cells  
954 (right panel) were transfected with either FLAG- or Myc-tagged MAML1 or E6AP, alone or in combination  
955 with HA-tagged HPV-16 E6 or HPV-8 E6. After 24hrs cells were harvested and isolated proteins from  
956 complete cell lysates separated on SDS-page, detected by anti-HA, anti-FLAG and anti-Myc antibodies and  
957 visualized by chemiluminescence. B-galactosidase (LacZ) was used as the control to monitor transfection  
958 efficiency and loading.

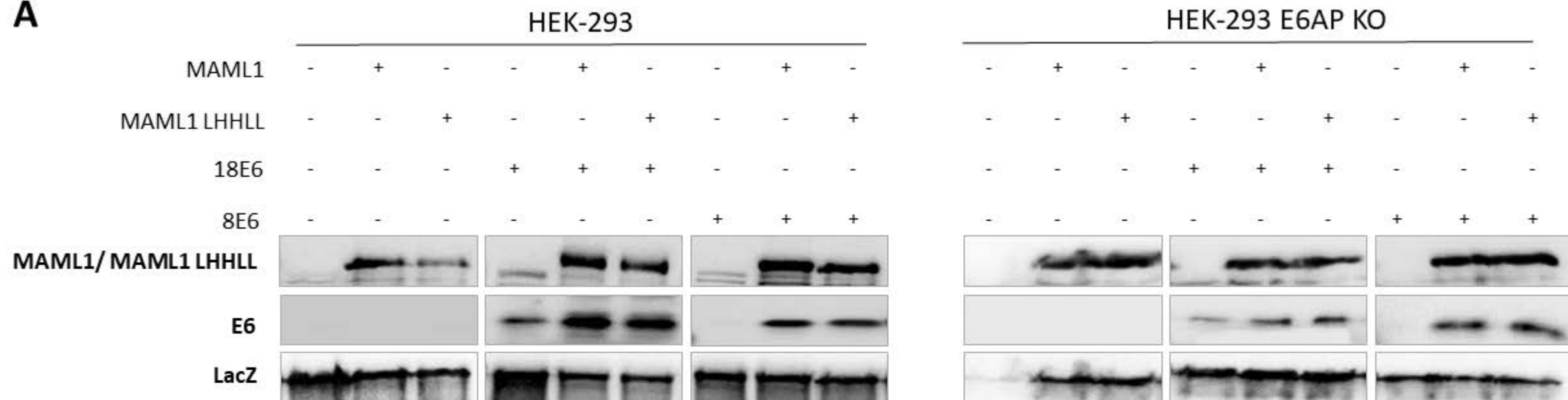
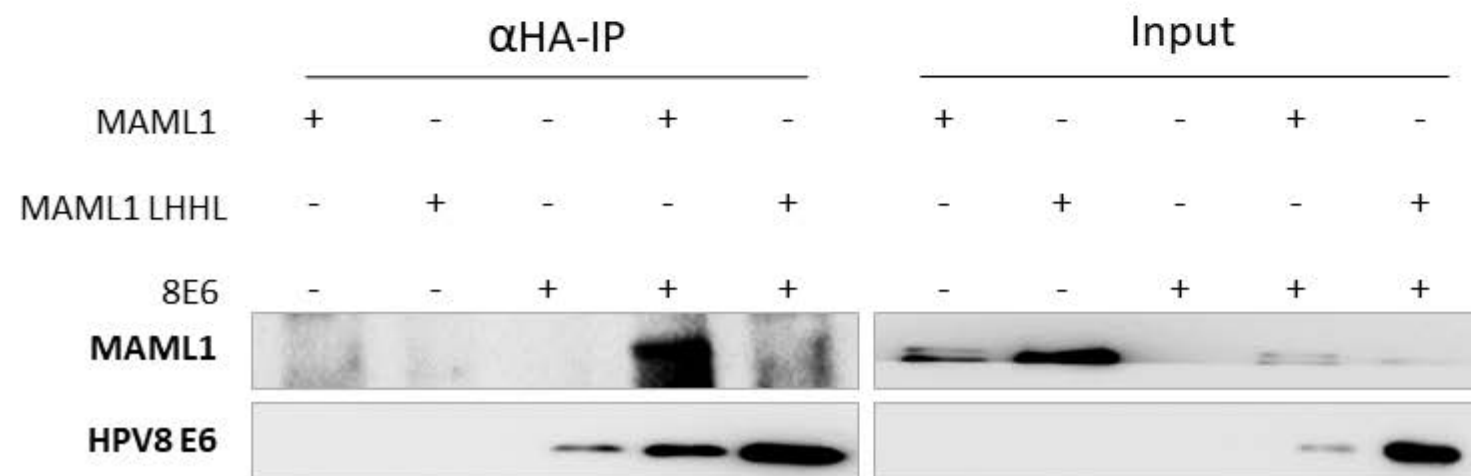
959 **Supp. Fig. 2. Negative controls for Figure 3.** (A) HEK-293 (left panel) and HEK-293 E6AP KO cells  
960 (right panel) were transfected with Myc-tagged MAML1 or Myc-tagged MAML1 mutant (MAML1 LHHLL),  
961 alone or in combination with HA-tagged HPV18 E6 or HPV-8 E6. After 24hrs cells were harvested and

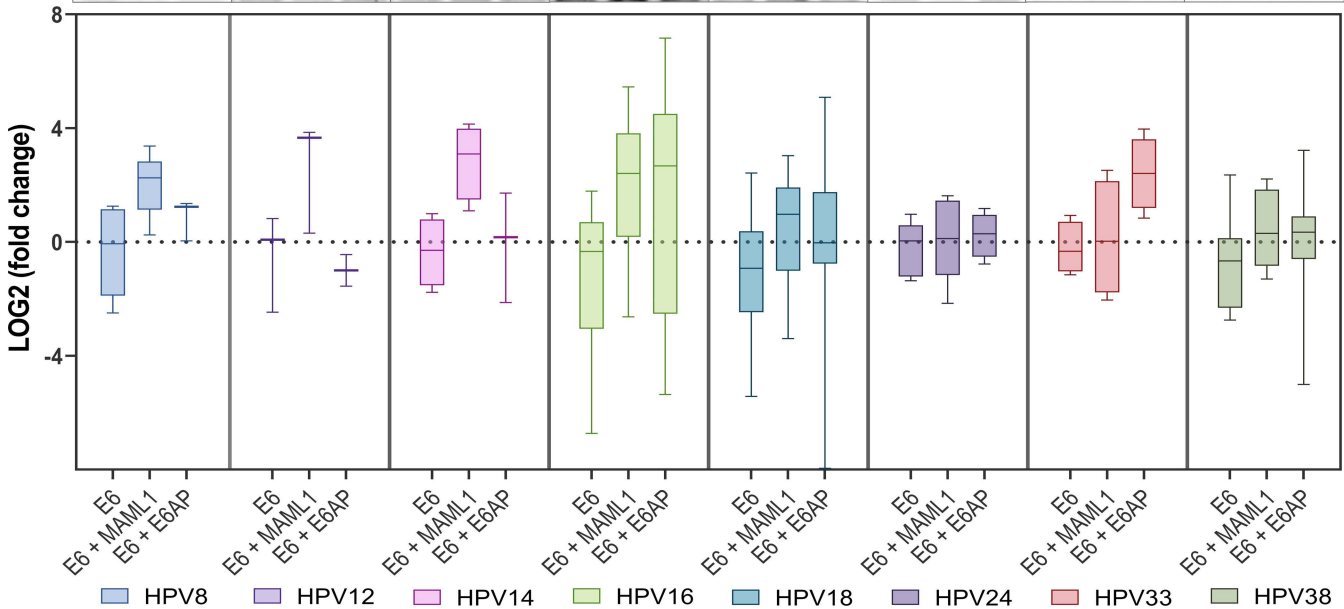
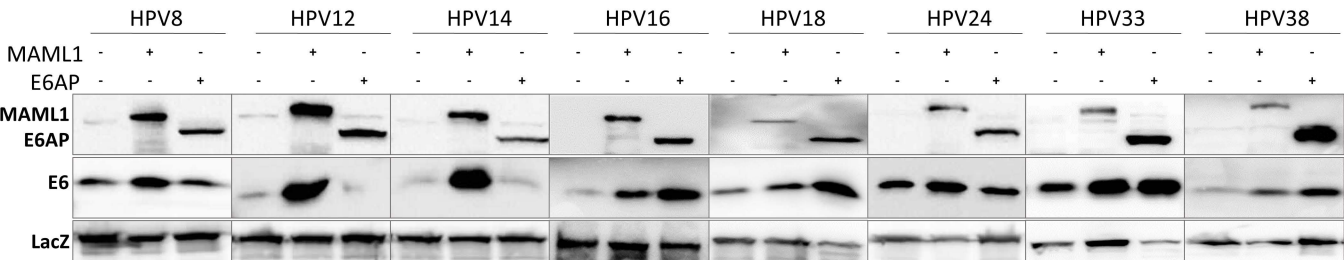
962 isolated proteins from complete cell lysates were separated on SDS-page and analyzed by western Blotting.  
963 MAML1 and MAML1 LHHLL were detected by anti-Myc antibodies, while HPV-8 E6 was detected with an  
964 anti-HA antibody. B-galactosidase (LacZ) was used as the control for the transfection efficiency and loading.  
965 (B) HEK-293 cells were transfected with either an empty plasmid, Myc-tagged MAML1, FLAG-tagged  
966 MAML1 LHHLL mutant and HA-tagged HPV-8 E6 alone or in combination. Twenty-four hrs post transfection  
967 the cells were harvested, resuspended in lysis buffer and incubated with anti-HA beads on a rotating wheel  
968 overnight at 4°C. The beads were extensively washed and co-immunoprecipitated complexes subjected to  
969 western blot analysis with anti-myc, anti-FLAG anti-HA-HRP antibodies and compared to the amount of  
970 MAML1, MAML1 LHHLL or 8 E6 present in 10% of the input.

971





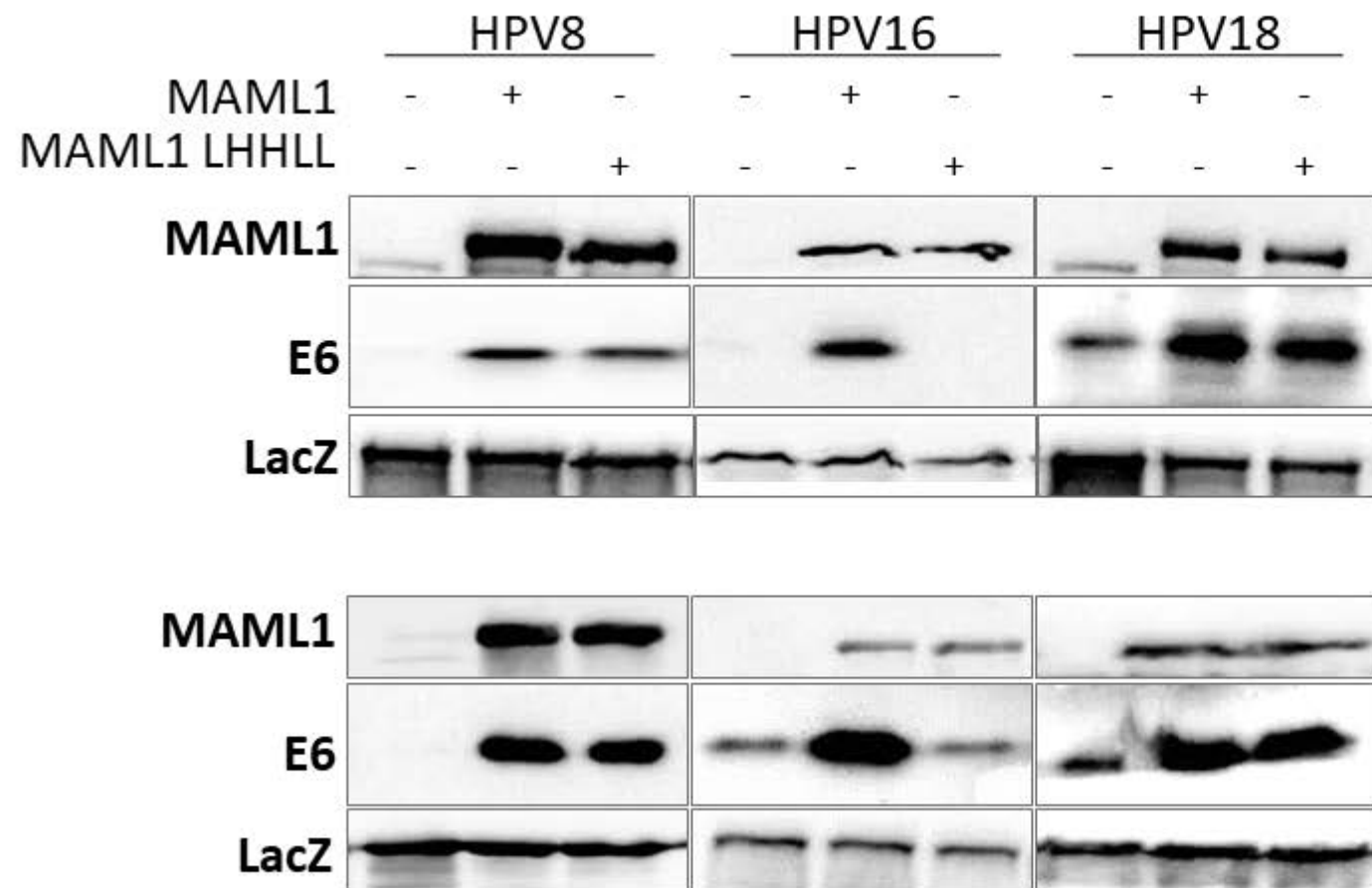
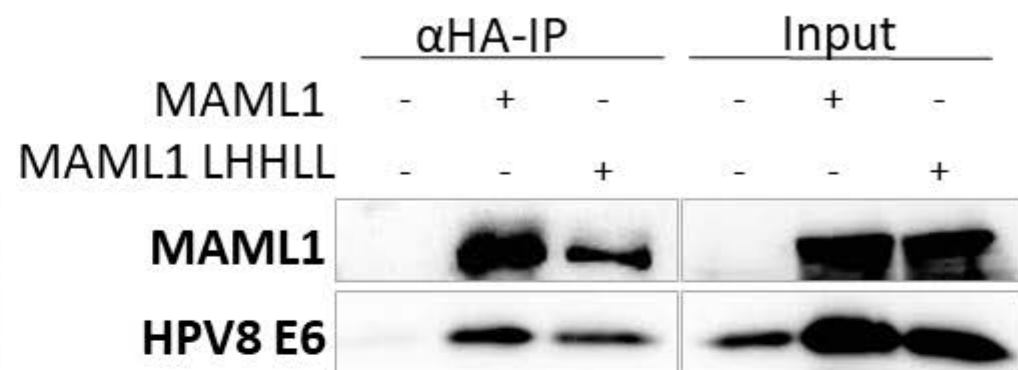
**A****B**

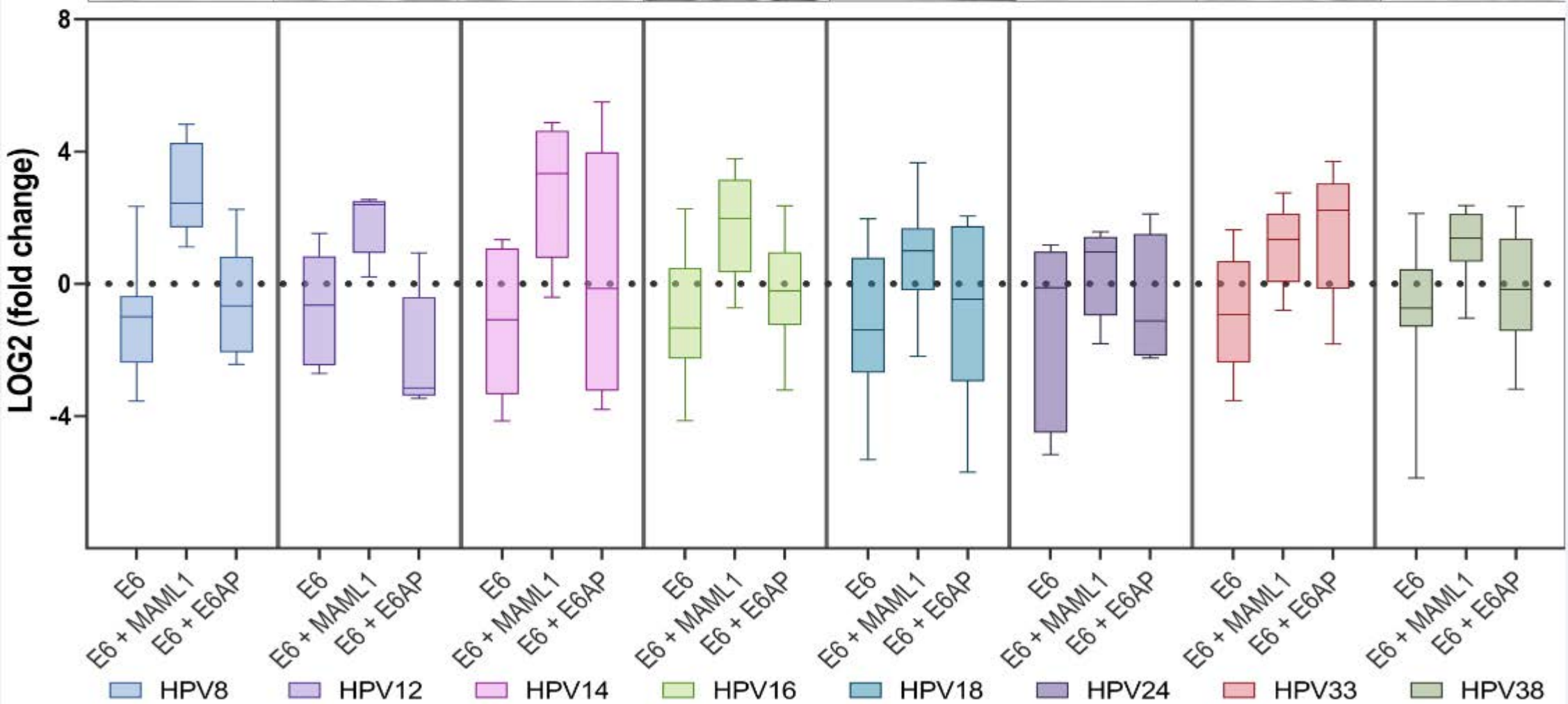
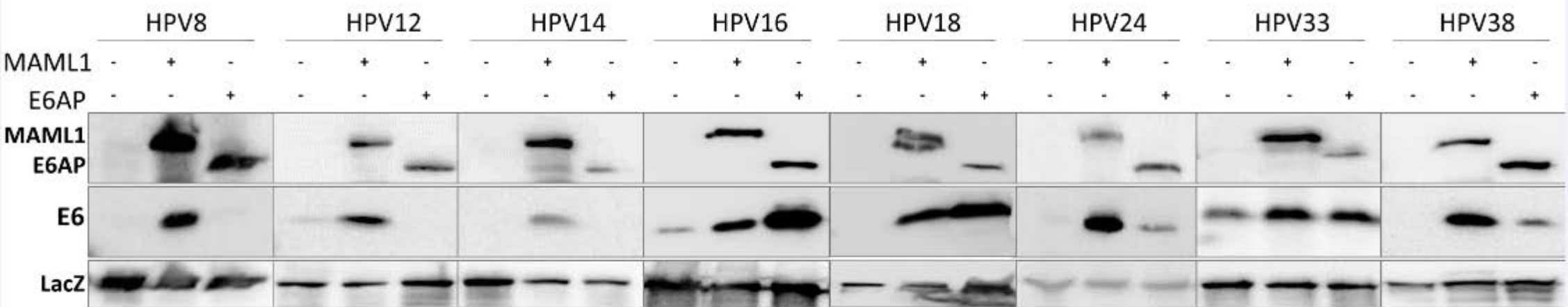


**A**

HEK-293

HEK-293 E6AP KO

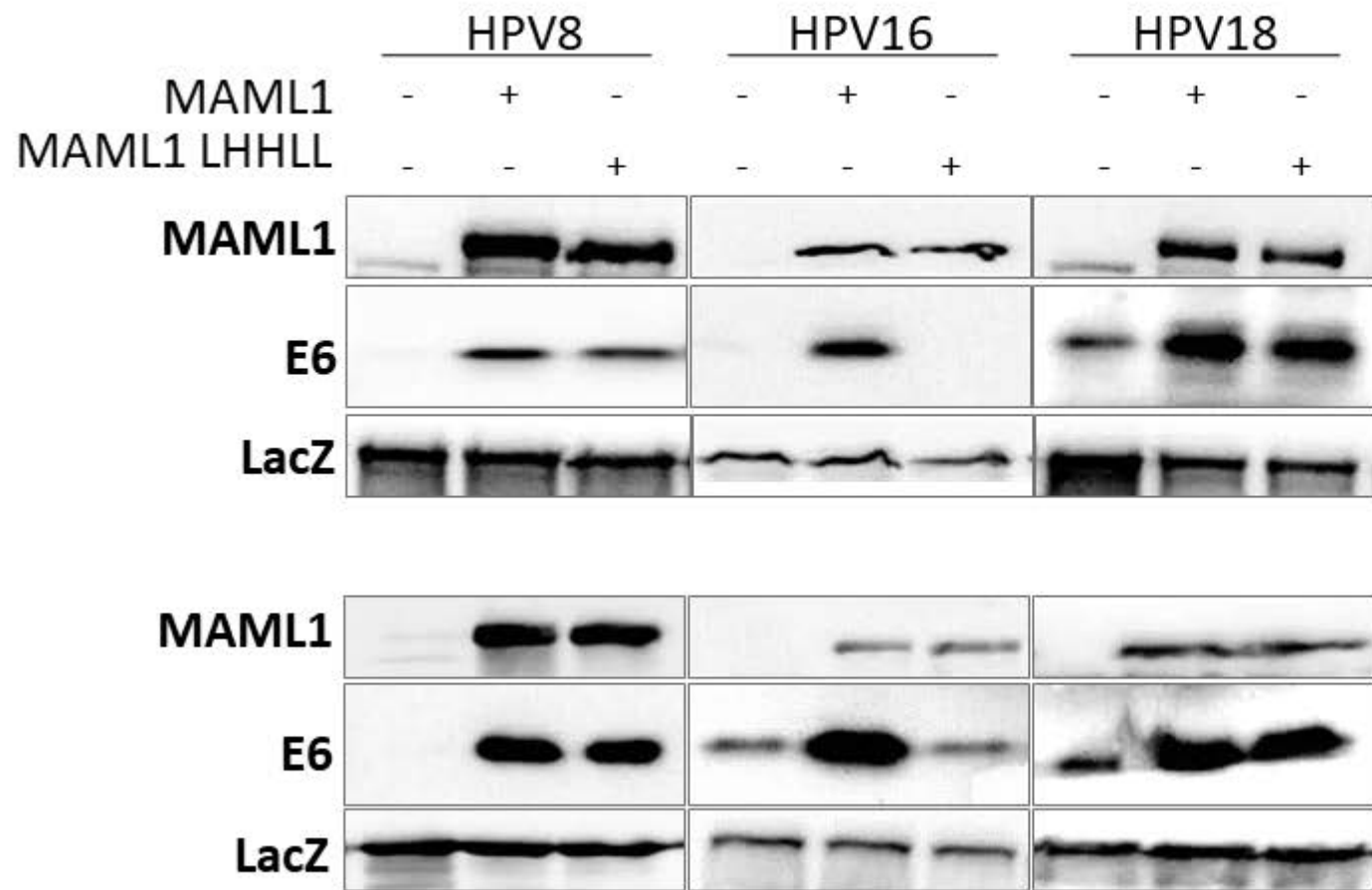
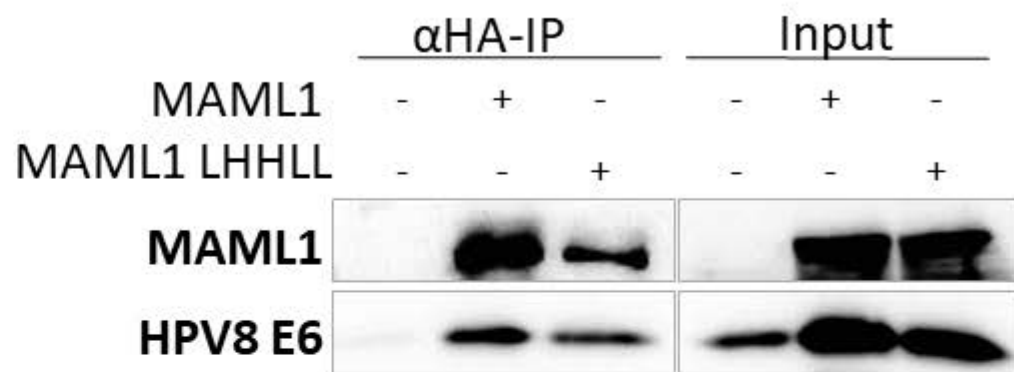
**B**

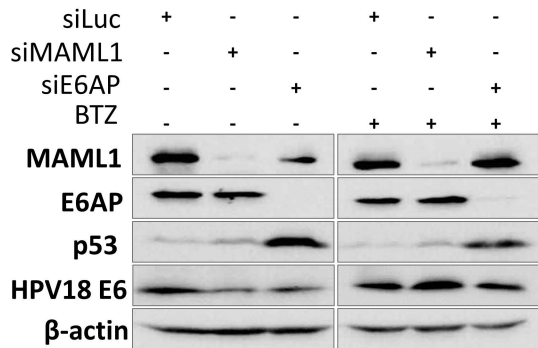
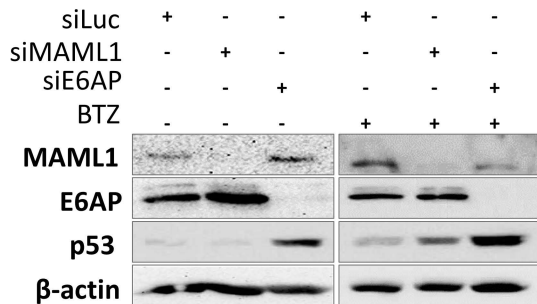
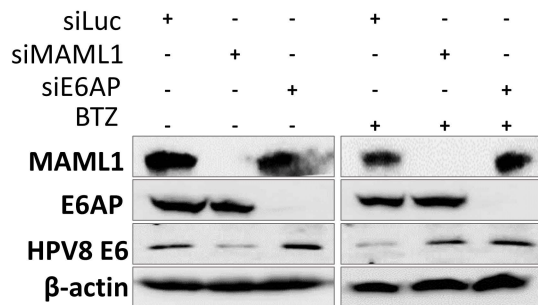


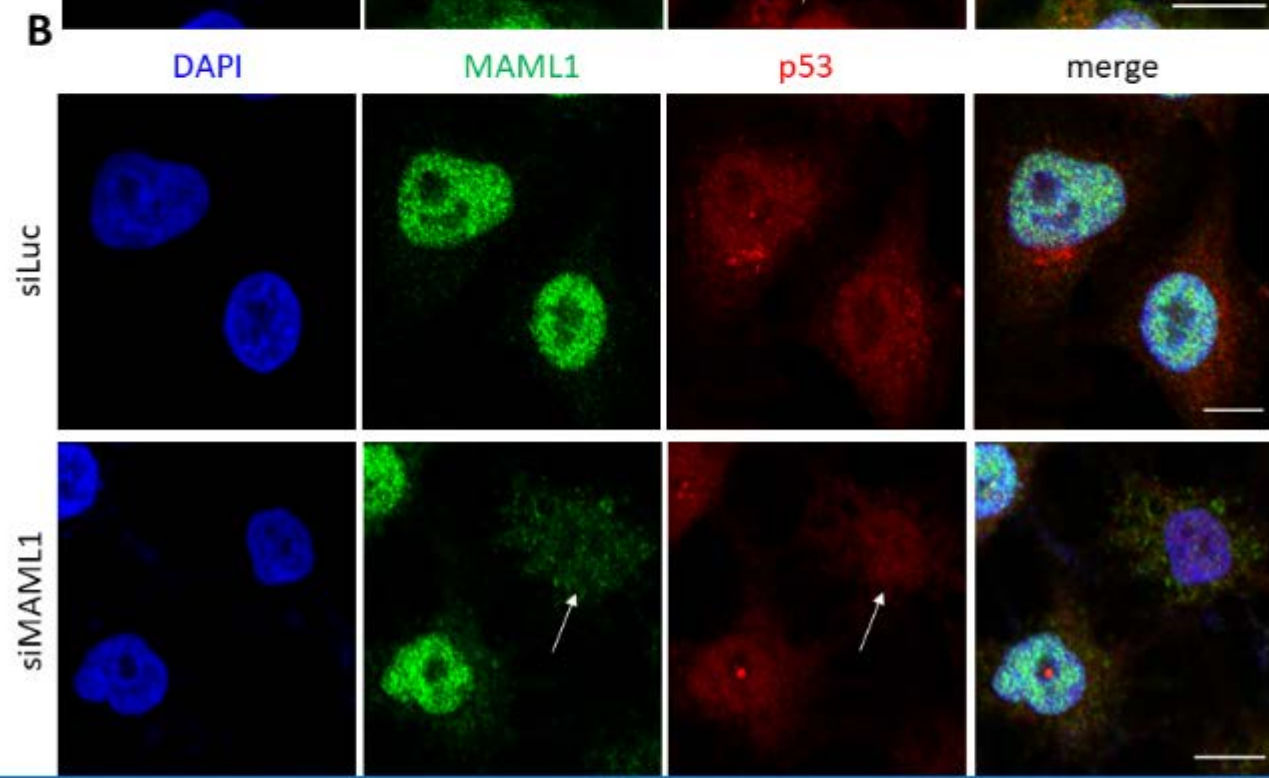
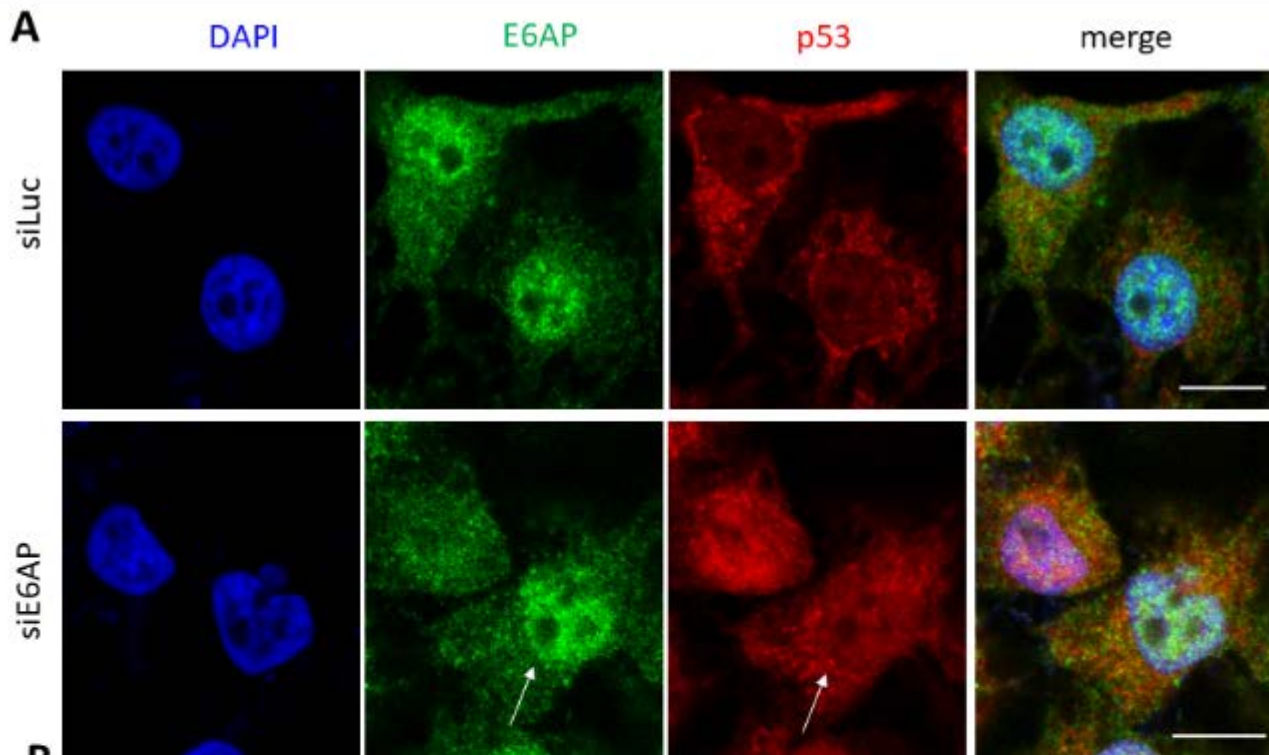
**A**

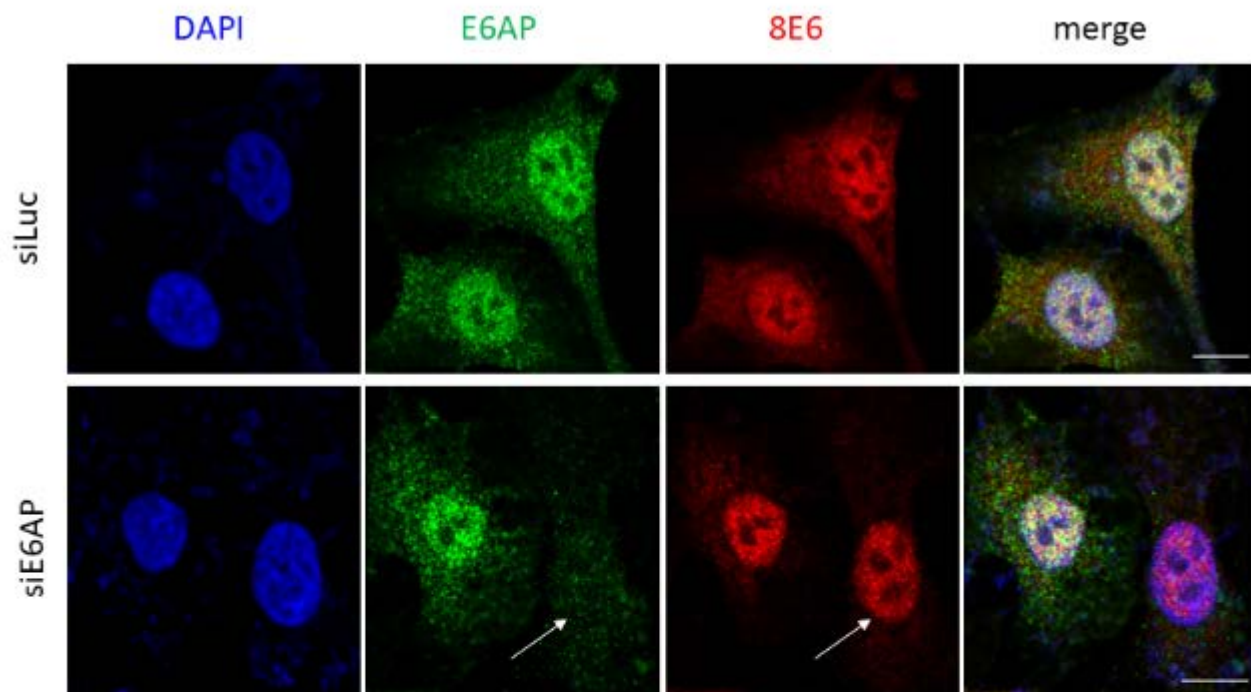
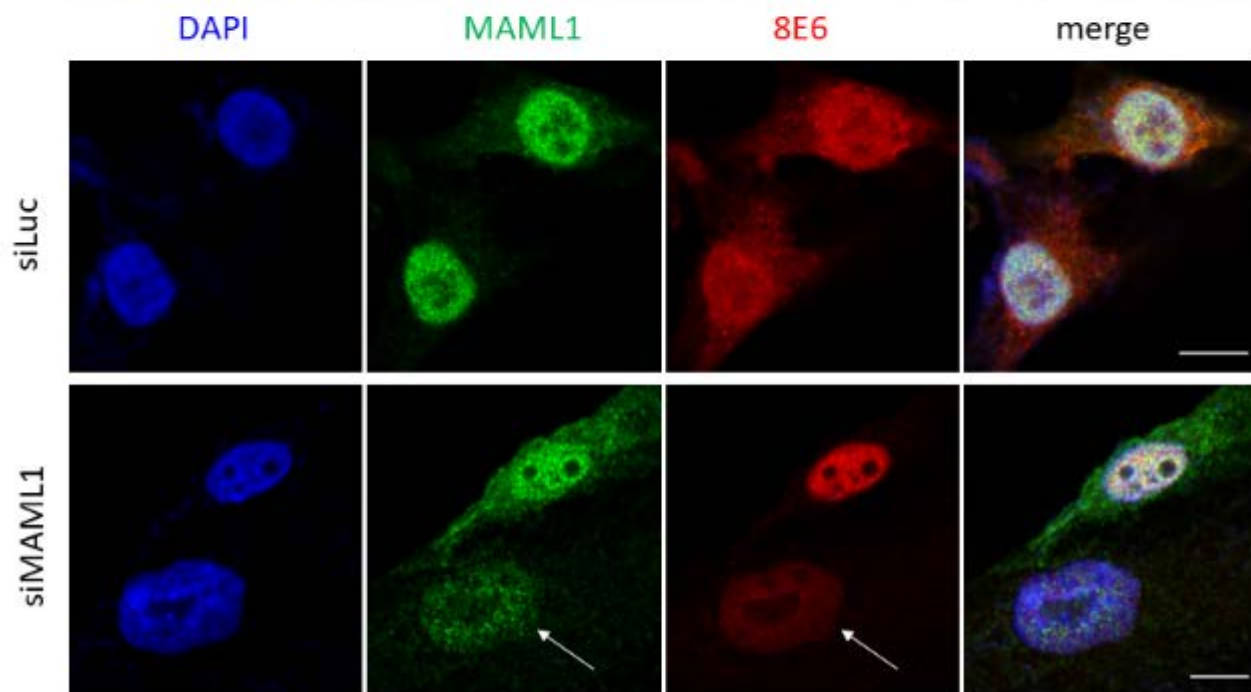
HEK-293

HEK-293 E6AP KO

**B**

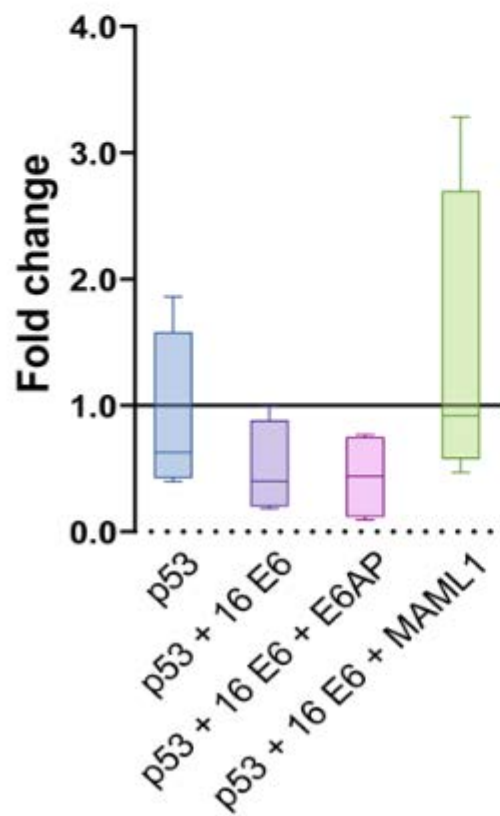
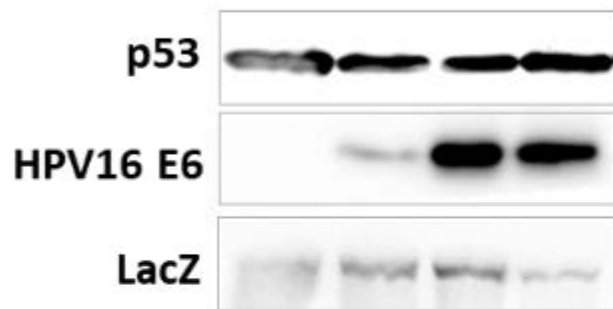
**A****B****C**



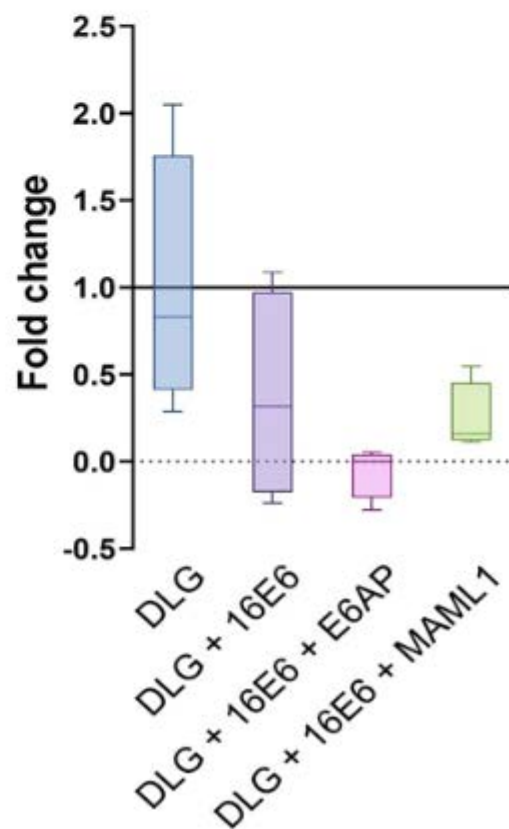
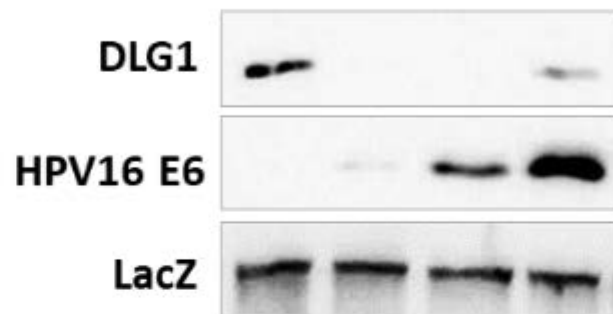
**C****D**

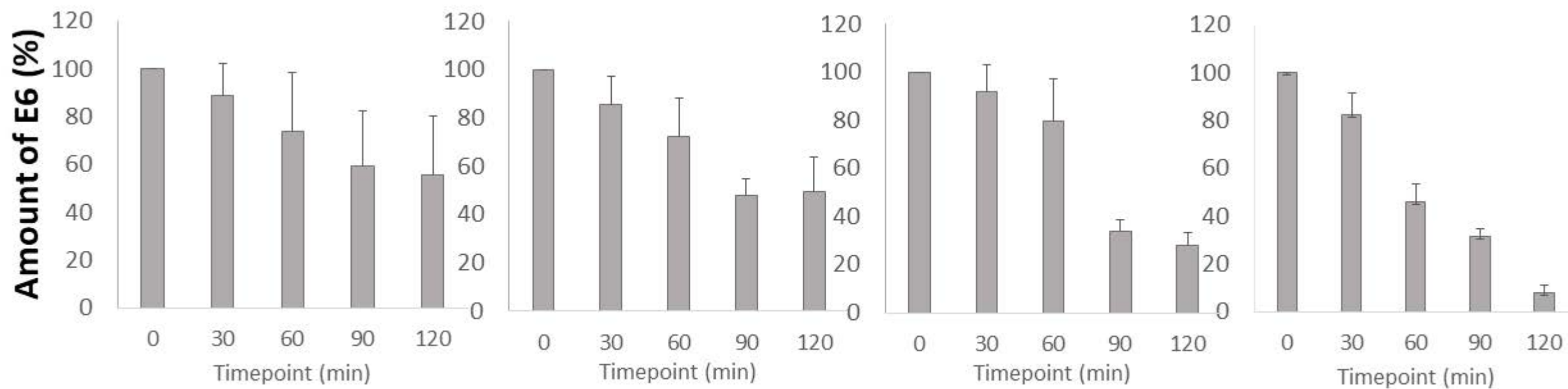
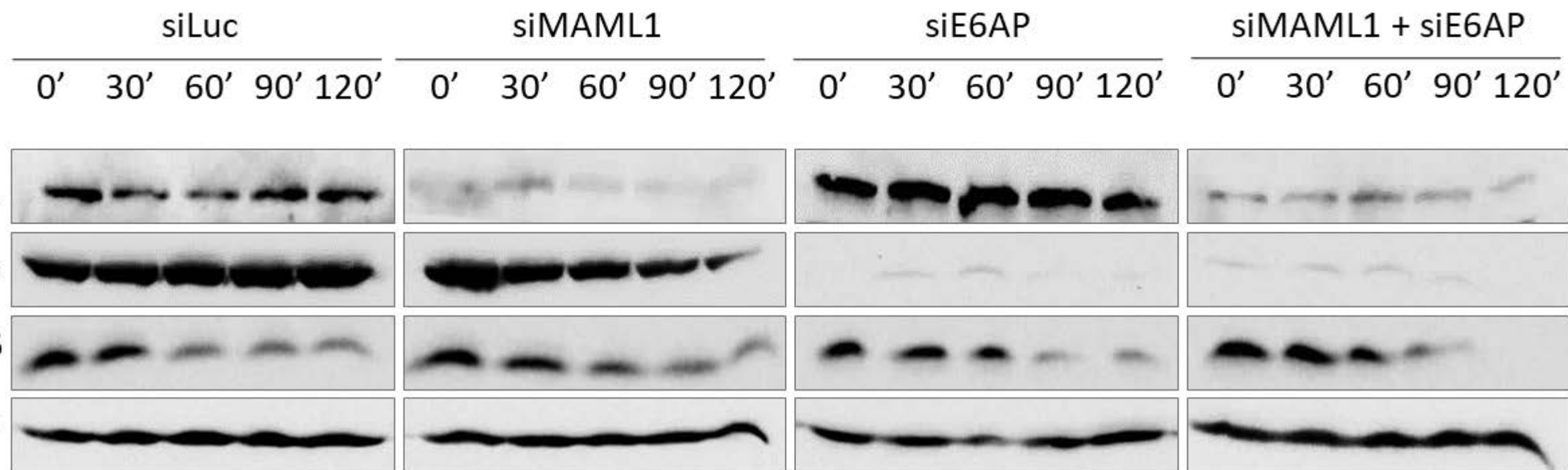
**A**

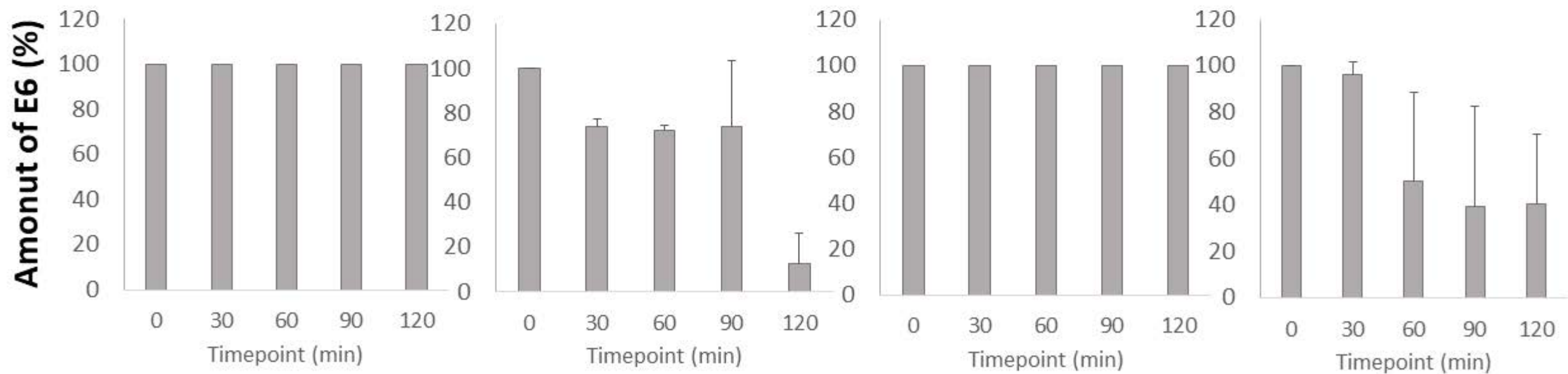
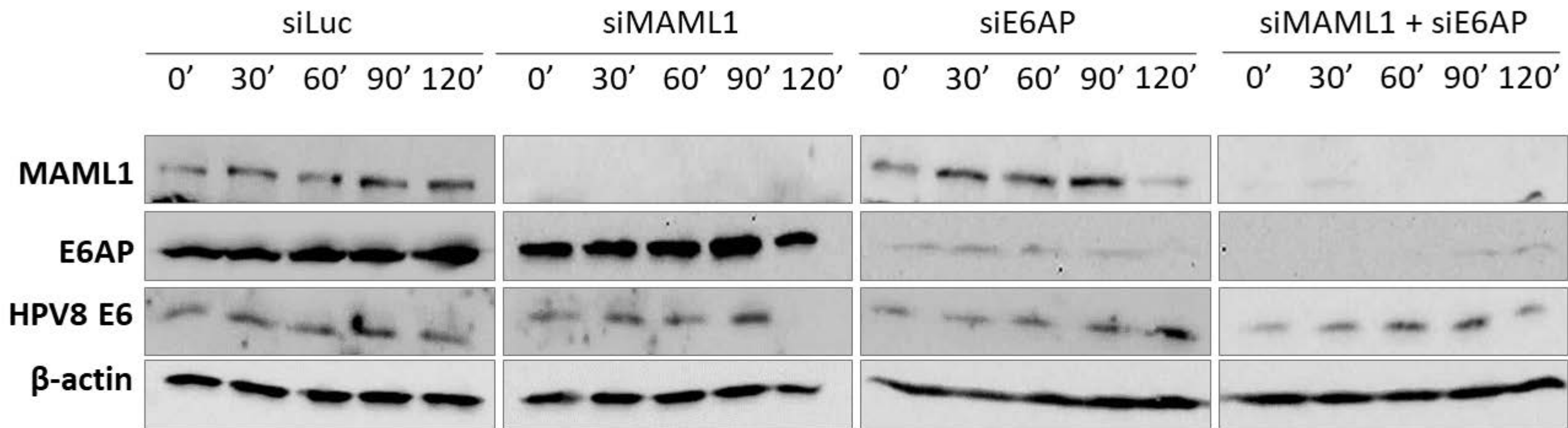
MAML1	-	-	-	+
E6AP	-	-	+	-
HPV16 E6	-	+	+	+

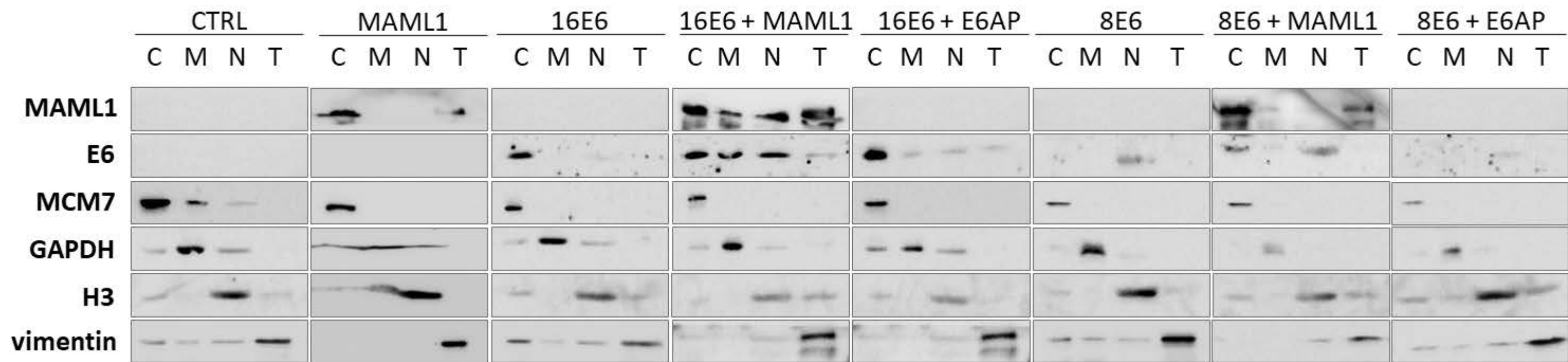
**B**

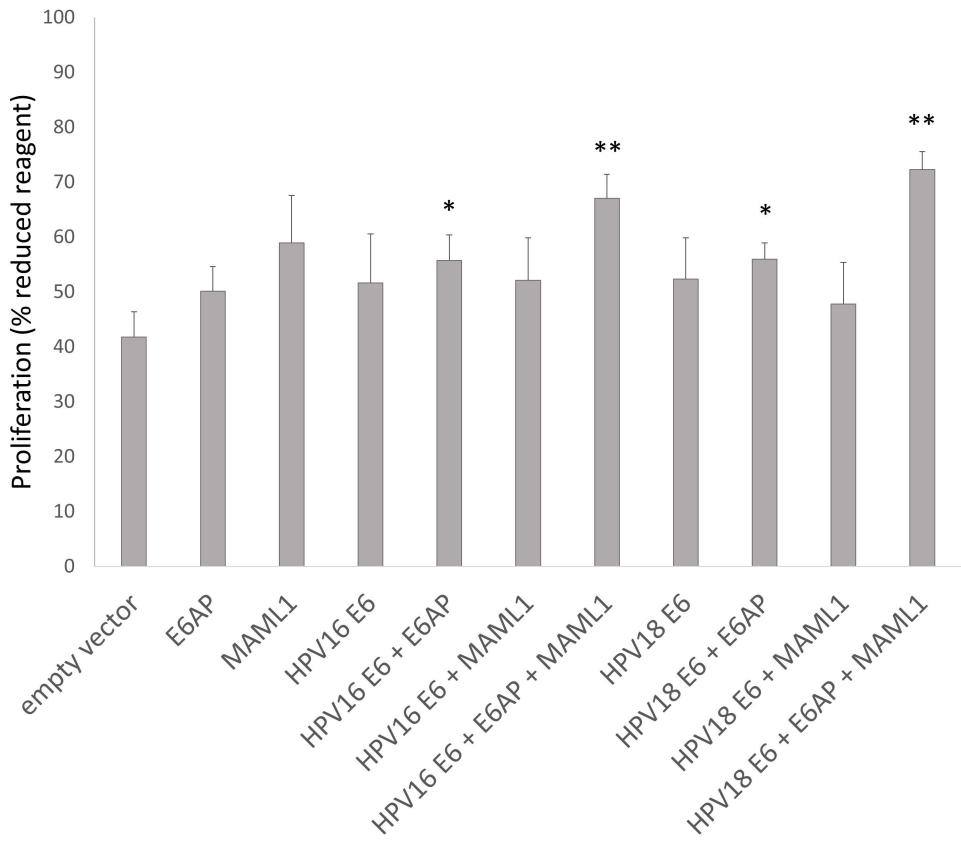
MAML1	-	-	-	+
E6AP	-	-	+	-
HPV16 E6	-	+	+	+







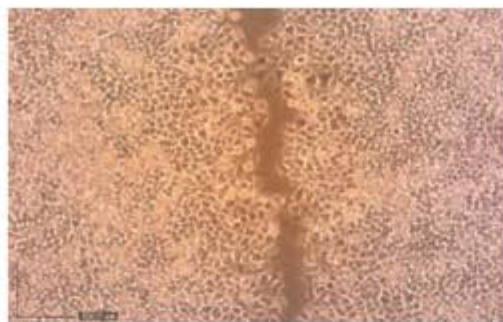
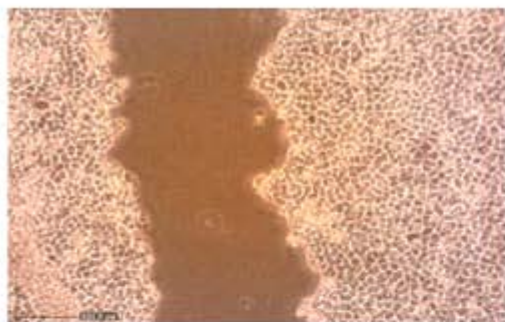




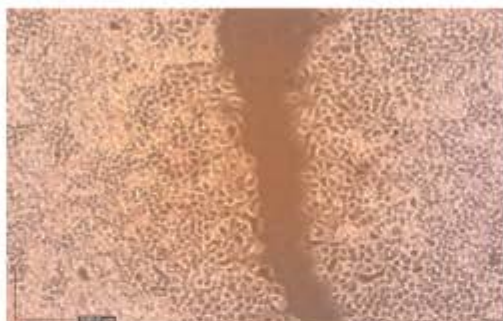
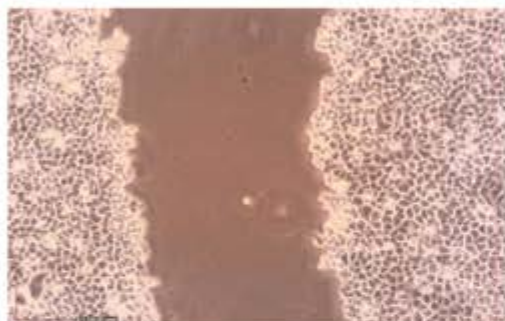
Initial scratch

18hrs later

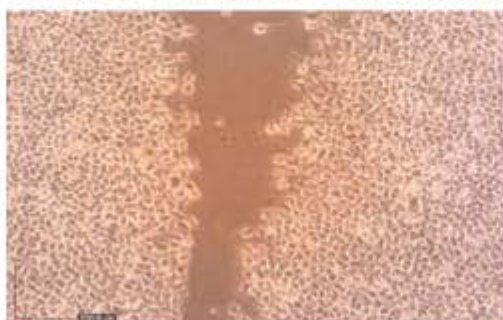
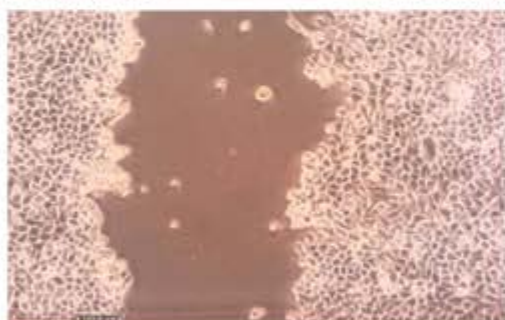
siLuc



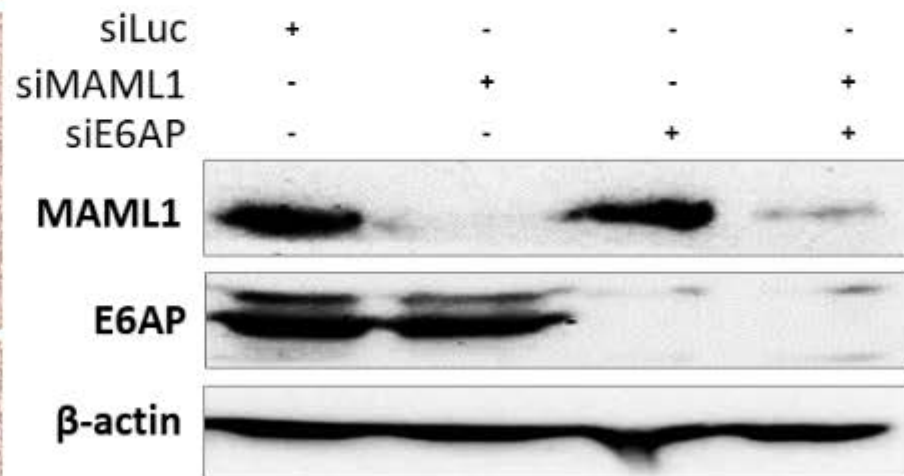
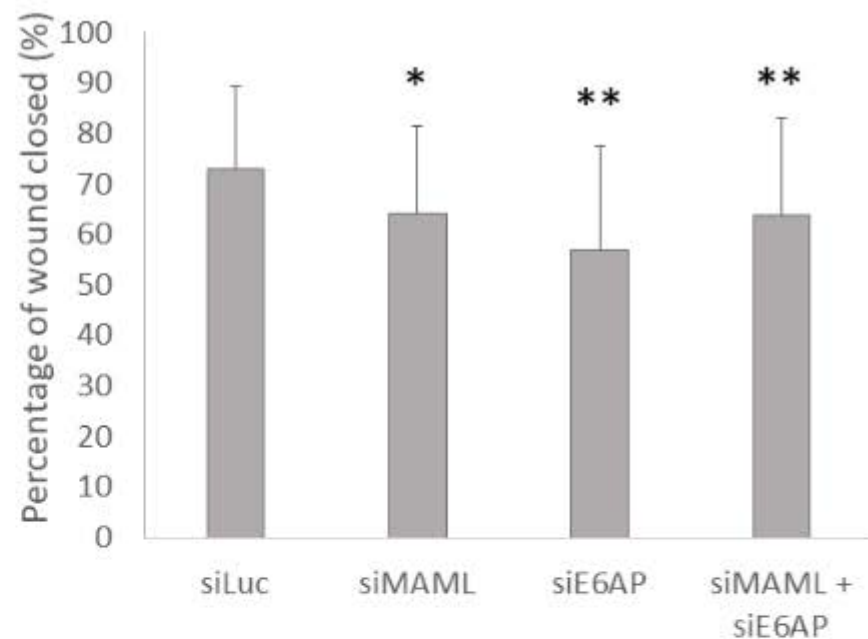
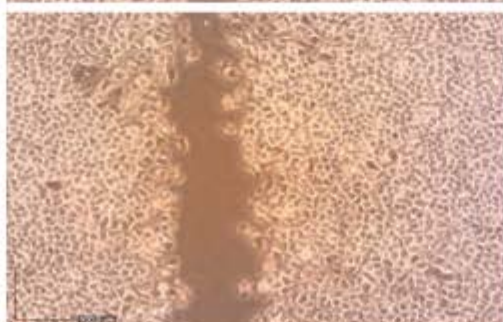
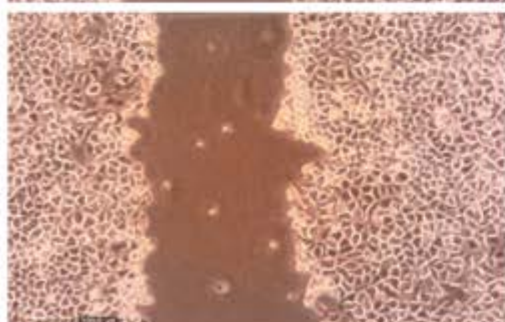
siMAML1



siE6AP



siMAML1 + siE6AP



$\alpha$ -HPV

$\beta$ -HPV

MAML1  
E6

E6AP  
E6

E6AP  
E6

MAML1  
E6

E6AP  
E6

MAML1  
E6

MAML1  
E6

MAML1  
E6

E6AP

E6AP

E6 stability

Migration

No effect on target  
degradation

E6 stability

Proliferation

Migration

Target  
degradation

E6 stability